

Regularized Estimation of Kronecker-Structured Covariance Matrix With Applications to Polarization Space-Time Adaptive Processing

Lei Xie, Zishu He, Jun Tong, Tianle Liu, Jun Li and Jiangtao Xi

Abstract—This paper investigates regularized estimation of Kronecker-structured covariance matrices (CM) for complex elliptically symmetric (CES) data. To obtain a well-conditioned estimate of the CM, we add penalty terms of Kullback-Leibler divergence to the negative log-likelihood function of the associated complex angular Gaussian (CAG) distribution. This is shown to be equivalent to regularizing Tyler’s fixed-point equations by shrinkage. A sufficient condition that the solution exists is discussed. An iterative algorithm is applied to solve the resulting fixed-point iterations and its convergence is proved. In order to solve the critical problem of tuning the shrinkage factors, we then introduce three methods by exploiting oracle approximating shrinkage (OAS) and cross-validation (CV). The proposed algorithms are applied to the CM estimation for polarization-space-time adaptive processing (PSTAP) in the context of heterogeneous clutter, where the clutter can be modeled using CES distributions with a Kronecker product-structured CM. When the training samples are limited, the proposed estimator, referred to as the robust shrinkage Kronecker estimator (RSKE), has better performance compared with several existing methods. Simulations are conducted for validating the proposed estimator and demonstrating its high performance.

Index Terms—Cross validation, complex elliptically symmetric distribution, shrinkage estimation, covariance matrix estimation, Kronecker product structure.

I. INTRODUCTION

COVARIANCE matrix (CM) estimation is a fundamental problem in many fields, such as adaptive detection and remote sensing [1]–[6]. The most common CM estimator is the sample covariance matrix (SCM), which is the maximum likelihood estimator (MLE) of the CM for Gaussian data. However, the SCM suffers poor performance for data with outliers or heavily-tailed distributions due to the lack of robustness. Such data are common in many applications [7]–[9] and often they can be described by complex elliptically symmetric (CES) distributions [10]. For instance, a subclass of CES distributions known as the compound-Gaussian (CG) distributions have been widely used in modeling the clutter

returns in radar applications [11]–[14]. To tackle the heavily-tailed data, one class of approaches is to censor the training samples with the aim to exclude outliers from the CM estimation [15]–[22]. Another class of methods is based on robustification. In particular, for CES distributions, various robust CM estimators based on the M-estimator have been developed and characterized [23]–[29]. With such estimators, outlying training samples are usually given small weights when an estimate of the CM is produced.

The SCM also requires an abundant number of samples to achieve satisfactory performance. Many modern applications involve high-dimensional variables whose statistical characteristics remain stationary over a short observation period, where the large sample support assumption does not hold. Regularization provides an effective strategy to improve the CM estimation for addressing the challenge of training shortage. In particular, a class of linear shrinkage algorithms have been introduced [30]–[33] and their integration into robust CM estimators for CES-distributed data have been thoroughly investigated in the recent works [34]–[37]. These algorithms estimate the CM by shrinking an estimate of the CM $\hat{\Sigma}$ toward a better-conditioned target matrix \mathbf{T} . There can be various choices for $\hat{\Sigma}$ and \mathbf{T} . For example, one can choose $\hat{\Sigma}$ as the SCM and Tyler’s estimator [25] for the Gaussian and non-Gaussian data, respectively. Moreover, different types of target matrices \mathbf{T} can be used, including the identity and diagonal targets. The linear shrinkage estimators can reduce the requirement of samples and provide positive-definite CM estimates. The choice of shrinkage factors is a fundamental problem for shrinkage estimators. Various criteria and methods have been studied. In particular, Ledoit and Wolf (LW) propose an approach that asymptotically minimizes the mean squared error (MSE) [31]. Then [33] improves the LW approach using the Rao-Blackwell theorem and designs the Rao-Blackwell Ledoit and Wolf (RBLW) estimator. The oracle approximating shrinkage (OAS) method is proposed in [33]. Both estimators have close-form expressions and are easily computed. The problem of determining the shrinkage factors can also be cast as a model selection problem and thus generic model selection techniques such as cross-validation (CV) [38] can be applied. The main challenges faced by CV include the choice of the cost function and the heavy computational cost in its direct implementation. Some efforts are made in [39], [40] to address these challenges for linear shrinkage estimators with unstructured CM.

Exploiting the structural knowledge about the CM can also

L. Xie, Z. He and J. Li are with the School of Information and Communication Engineering, University of Electronic Science and Technology of China, Chengdu 611731, China (e-mail: leixie123@hotmail.com).

J. Tong and J. Xi are with the School of Electrical, Computer, and Telecommunications Engineering, University of Wollongong, Wollongong, NSW 2522, Australia.

T. Liu is with the School of Communications Engineering, Hangzhou Dianzi University, Hangzhou 310018, China.

This work was supported by the National Natural Science Foundation of China under Grants 61671139 and 61771095.

significantly reduce the number of unknown parameters and improve its high estimation accuracy under limited training data [41]–[51]. Kronecker-structured CM is widely seen in many scenarios such as modeling multiple-input multiple-output (MIMO) wireless communication channels [52]–[54] and the clutter in polarization-space-time adaptive processing (PSTAP) [55]–[58]. Particularly, [41] proposes a robust estimator for Kronecker-structured CM and proves that a globally optimal solution can be found, [42] proposes a majorization minimization (MM) solution to the Kronecker maximum likelihood estimator (KMLE), and [59] introduces the maximum likelihood (ML) estimation of Kronecker-structured CM with the presence of Gaussian clutter. An extension of KMLE is also studied for compound Gaussian clutter with inverse Gamma-distributed texture and Kronecker normalized sample covariance matrix (KNSCM) is proposed in [60] to estimate the CM. Both KMLE and KNSCM provide considerable performance with sufficient samples but they can still noticeably suffer performance degradation with low sample supports.

A. Contributions

In this paper, we consider the estimation of Kronecker-structured CM for CES data under low sample supports. We investigate a robust shrinkage Kronecker estimator (RSKE) that aims to achieve well-conditioned¹ and highly accurate CM estimates. With RSKE, the structural knowledge is exploited together with robustification and regularization techniques. Based on the findings of the previous studies in [10], [34], [36], [39], [62], [63] and others, we investigate the existence of RSKE, its iterative solver and convergence, and also the choice of the shrinkage factors. We also study the performance of the RSKE for the polarization space-time adaptive processing (PSTAP) in radar applications. The contributions of this paper can be summarized as follows:

- 1) We show that the RSKE can be interpreted as the minimizer of a negative log-likelihood function penalized by the Kullback-Leibler divergence. Based on this, the condition for the existence of RSKE is established under some mild assumptions, which provides insights to the relationship between the dimensionality, sample size and shrinkage factors.
- 2) We study an iterative solver involving two fixed-point equations to find RSKE and prove its convergence. Following the majorization-minimization framework, we prove the monotonic decrease of the penalized log-likelihood function over iterations. We show that, with fixed shrinkage factors and arbitrary positive-definite initial matrices, the iterative solver converges.
- 3) We address the critical challenge of shrinkage factor choice in order to exploit the potential of RSKE. We introduce data-driven methods that automatically tune the linear shrinkage factors, based on oracle approximating shrinkage (OAS) and cross-validation (CV). The OAS method adopts a minimum MSE (MMSE) criterion

and plug-in estimates of the oracle shrinkage factors. For the CV methods, we start with a quadratic loss for leave-one-out CV (LOOCV) and derive analytical solutions of the shrinkage factors which can approach the performance of the oracle solutions that minimize the MSE of CM estimation. The complexities of these different methods are analyzed. We show that they exhibit different complexities, performance, and require different levels of a prior knowledge and thus may be useful in different scenarios. Note that one main challenge of the CV is its computational cost. However, the proposed CV-based methods have close-form expressions for the shrinkage factors which can address this challenge. Owing to such expressions, the complexity of the CV-based RSKE is about the same as that of the KMLE.

- 4) We demonstrate the application of the RSKE to PSTAP. We investigate the effectiveness of RSKE in addressing the heterogeneous training samples of radar clutter. Numerical studies are reported to show the performance of RSKE relative to several existing estimators.

B. Organization

The remainder of this paper is organized as follows. Section II introduces the RSKE, its existence and iterative solution. Section III gives the choices of the shrinkage factors. Section IV introduces the application to polarization space-time clutter suppression. Section V presents simulation results to show the performance of CM estimation. Finally, Section VI gives the conclusions.

II. ROBUST SHRINKAGE KRONECKER ESTIMATOR (RSKE)

In this section, we introduce the robust shrinkage estimator for Kronecker-structured covariance matrices. We first discuss the motivation, then discuss the condition for its existence, and finally introduce the iterative solver and its convergence property.

A. Motivation

Let \mathbf{y} be an N -dimensional zero-mean random vector following a CES distribution, whose probability density function (p.d.f.) is of the form [10], [29],

$$p(\mathbf{y}) = C_{N,g} \det(\mathbf{R})^{-1} g(\mathbf{y}^H \mathbf{R}^{-1} \mathbf{y}), \quad (1)$$

where $(\cdot)^H$ is the conjugate transpose, $g(\cdot)$ denotes the density generator, $C_{N,g}$ a normalizing constant, and \mathbf{R} the normalized covariance matrix with its trace $\text{Tr}(\mathbf{R}) = N$. Note that \mathbf{R} is also known as the scatter matrix [10], [29]. We consider the case that \mathbf{R} can be expressed as the Kronecker product of two matrices, i.e., $\mathbf{R} \triangleq \mathbf{R}_A \otimes \mathbf{R}_B$, where $\mathbf{R}_A \in \mathbb{S}_{++}^{N_A}$, $\mathbf{R}_B \in \mathbb{S}_{++}^{N_B}$, \otimes denotes the Kronecker product, and \mathbb{S}_{++}^n denotes the set of Hermitian, positive definite matrices of size $n \times n$. In order to define \mathbf{R}_A and \mathbf{R}_B uniquely, we assume $\text{Tr}(\mathbf{R}_A) = N_A$ and $\text{Tr}(\mathbf{R}_B) = N_B$, which is consistent with the assumption $\text{Tr}(\mathbf{R}) = N$.

¹For a positive-definite, Hermitian matrix, the condition number is defined as the ratio of its maximum and minimum eigenvalues [61]. A well-conditioned matrix indicates that its condition number is small.

This paper considers the estimation of \mathbf{R} from $\mathcal{Y} = \{\mathbf{y}_l\}_{l=1}^L$ which is a set of independent and identically distributed (i.i.d.) samples of \mathbf{y} . The normalized samples $\{\mathbf{x}_l = \frac{\mathbf{y}_l}{\|\mathbf{y}_l\|}\}_{l=1}^L$, which belong to a complex unit N -dimensional sphere, follows the complex angular Gaussian (CAG) distribution [10], [29]. The joint distribution function of $\{\mathbf{x}_l\}_{l=1}^L$ is expressed as [10]

$$p(\{\mathbf{x}_l\}) = \prod_{l=1}^L p(\mathbf{x}_l) \propto \det(\mathbf{R})^{-L} \prod_{l=1}^L (\mathbf{x}_l^H \mathbf{R}^{-1} \mathbf{x}_l)^{-N}, \quad (2)$$

where $\det(\cdot)$ denotes the determinant. After omitting some additive constants and scaling, the negative log-likelihood function of such a joint distribution is given by

$$\begin{aligned} \mathcal{L}_0(\hat{\mathbf{R}}_A, \hat{\mathbf{R}}_B) &= \log \det(\hat{\mathbf{R}}_A \otimes \hat{\mathbf{R}}_B) \\ &+ \frac{N}{L} \sum_{l=1}^L \log \mathbf{y}_l^H (\hat{\mathbf{R}}_A \otimes \hat{\mathbf{R}}_B)^{-1} \mathbf{y}_l, \end{aligned} \quad (3)$$

where $\hat{\mathbf{R}}_A \in \mathbb{S}_{++}^{N_A}$, $\hat{\mathbf{R}}_B \in \mathbb{S}_{++}^{N_B}$ and we have used the fact that $\log(\mathbf{y}_l^H \hat{\mathbf{R}}^{-1} \mathbf{y}_l) - \log(\mathbf{x}_l^H \hat{\mathbf{R}}^{-1} \mathbf{x}_l) = \log(\|\mathbf{y}_l\|^2)$ is irrelevant to $\hat{\mathbf{R}} = \hat{\mathbf{R}}_A \otimes \hat{\mathbf{R}}_B$ in the likelihood function. The above cost function $\mathcal{L}_0(\hat{\mathbf{R}}_A, \hat{\mathbf{R}}_B)$ is non-convex in the classical definitions but is jointly g-convex (geodesic-convex) with respect to $\hat{\mathbf{R}}_A$ and $\hat{\mathbf{R}}_B$ [41]. Minimizing this cost function produces the KMLE [42], [63]. In the low-sample-support cases, the solution of KMLE can suffer from significant errors and ill-conditioning. For many applications such as beamforming and spectral estimation [64]–[69], the inverse of the CM estimate is required. Inverting an erroneous, ill-conditioned CM estimate can bring enormous errors. This motivates the design of accurate, well-conditioned CM estimators.

B. Regularization via KL Divergence Penalty

In this subsection, we introduce a penalized estimator that promotes well-conditioned estimates of the sub-CMs \mathbf{R}_A and \mathbf{R}_B . We adopt penalty terms of the Kullback-Leibler divergence for Gaussian distributions [70], i.e.,

$$D_{\text{KL}}(\mathbf{X}, \mathbf{Y}) = \text{Tr}(\mathbf{X}\mathbf{Y}^{-1}) - \log \det(\mathbf{X}\mathbf{Y}^{-1}) - N,$$

where $\mathbf{X}, \mathbf{Y} \in \mathbb{S}_{++}^N$. As shown in [71], the KL divergence $D_{\text{KL}}(\mathbf{X}, \mathbf{I}_N)$ can effectively constrain the condition number of \mathbf{X} . We thus add the penalty terms $\alpha_A D_{\text{KL}}(\hat{\mathbf{R}}_A^{-1}, \mathbf{I}_{N_A})$ and $\alpha_B D_{\text{KL}}(\hat{\mathbf{R}}_B^{-1}, \mathbf{I}_{N_B})$ to the negative log-likelihood function in (3) to promote well-conditioned estimates $\hat{\mathbf{R}}_A$ and $\hat{\mathbf{R}}_B$, where $\alpha_A = \frac{N_B \rho_A}{1 - \rho_A}$ and $\alpha_B = \frac{N_A \rho_B}{1 - \rho_B}$ with $\rho_A \in [0, 1)$ and $\rho_B \in [0, 1)$. Ignoring some additive constants which are irrelevant to $\hat{\mathbf{R}}_A$ and $\hat{\mathbf{R}}_B$, the penalized negative log-likelihood function is obtained as

$$\begin{aligned} \mathcal{L}(\hat{\mathbf{R}}_A, \hat{\mathbf{R}}_B) &= \frac{N_B}{1 - \rho_A} \log \det(\hat{\mathbf{R}}_A) + \frac{N_A}{1 - \rho_B} \log \det(\hat{\mathbf{R}}_B) \\ &+ \frac{N}{L} \sum_{l=1}^L \log \mathbf{y}_l^H (\hat{\mathbf{R}}_A \otimes \hat{\mathbf{R}}_B)^{-1} \mathbf{y}_l + \frac{N_B \rho_A}{1 - \rho_A} \text{Tr}(\hat{\mathbf{R}}_A^{-1}) \\ &+ \frac{N_A \rho_B}{1 - \rho_B} \text{Tr}(\hat{\mathbf{R}}_B^{-1}), \end{aligned} \quad (4)$$

which reduces to $\mathcal{L}_0(\hat{\mathbf{R}}_A, \hat{\mathbf{R}}_B)$ in (3) when $\rho_A = \rho_B = 0$. By adding the penalty terms which are convex, the obtained objective function is also g-convex w.r.t. $\hat{\mathbf{R}}_A$ and $\hat{\mathbf{R}}_B$. This guarantees that all local minimizers of $\mathcal{L}(\hat{\mathbf{R}}_A, \hat{\mathbf{R}}_B)$ are also globally optimal, following [41, Proposition 1]. Minimizing the penalized log-likelihood function by setting $\partial \mathcal{L}(\hat{\mathbf{R}}_A, \hat{\mathbf{R}}_B) / \partial \hat{\mathbf{R}}_A = \mathbf{0}$ and $\partial \mathcal{L}(\hat{\mathbf{R}}_A, \hat{\mathbf{R}}_B) / \partial \hat{\mathbf{R}}_B = \mathbf{0}$ yields the fixed-point equations

$$\hat{\mathbf{R}}_A = (1 - \rho_A) \frac{N_A}{L} \sum_{l=1}^L \frac{\mathbf{Y}_l^H \hat{\mathbf{R}}_B^{-1} \mathbf{Y}_l}{\mathbf{y}_l^H (\hat{\mathbf{R}}_A^{-1} \otimes \hat{\mathbf{R}}_B^{-1}) \mathbf{y}_l} + \rho_A \mathbf{I}_{N_A}, \quad (5a)$$

$$\hat{\mathbf{R}}_B = (1 - \rho_B) \frac{N_B}{L} \sum_{l=1}^L \frac{\mathbf{Y}_l \hat{\mathbf{R}}_A^{-1} \mathbf{Y}_l^H}{\mathbf{y}_l^H (\hat{\mathbf{R}}_A^{-1} \otimes \hat{\mathbf{R}}_B^{-1}) \mathbf{y}_l} + \rho_B \mathbf{I}_{N_B}. \quad (5b)$$

In the above, we have defined

$$\begin{aligned} \mathbf{Y}_l &= \text{unvec}_{N_B N_A}(\mathbf{y}_l) \\ &\triangleq \begin{bmatrix} y_l^{(1)} & y_l^{(N_B+1)} & \cdots & y_l^{(N_B(N_A-1)+1)} \\ y_l^{(2)} & y_l^{(N_B+2)} & \cdots & y_l^{(N_B(N_A-1)+2)} \\ \vdots & \vdots & \ddots & \vdots \\ y_l^{(N_B)} & y_l^{(2N_B)} & \cdots & y_l^{(N_B(N_A-1)+N_B)} \end{bmatrix} \in \mathbb{C}^{N_B \times N_A}, \end{aligned} \quad (6)$$

where $y_l^{(i)}$ denotes the i th entry of \mathbf{y}_l and $\text{unvec}_{N_B N_A}(\cdot)$ reshapes a vector into a $N_B \times N_A$ matrix as shown above. Therefore, the solution to (5), if exists, can be interpreted as the minimizer of the penalized negative log-likelihood function (4). These fixed-point equations interestingly have the same form as the linear shrinkage estimators for unstructured CM [31], [33]–[37]. Following these work, we refer to the resultant CM estimator as the robust shrinkage Kronecker estimator (RSKE), with shrinkage factors ρ_A and ρ_B . The KMLE [42] can be obtained as a special case of RSKE by letting $\rho_A = \rho_B = 0$.

It should be noted that in [63], estimators that exploit robustification and shrinkage for the unstructured CM and robust estimators for the Kronecker-structured CM have been thoroughly studied via the geodesic convexity. The KL divergence penalty has also been exploited in [36] for robust estimation of unstructured CM. We here extend these studies to the estimation of Kronecker-structured CM by simultaneously exploiting robustification and shrinkage.

C. Existence of RSKE

In this subsection, we examine the conditions under which the RSKE exists. When ρ_A and ρ_B are small, it is possible that the cost function (4) tends to $-\infty$ on the boundary of the set $\mathbb{S}_{++}^{N_A}$ and $\mathbb{S}_{++}^{N_B}$, i.e., (4) becomes unbounded below and there is no solution to the fix-point equations of (5). The existence of the shrinkage Tyler's estimator for unstructured CM has been studied in [36], where the relationship between the shrinkage factors, sample size, and dimensionality is revealed. By establishing the condition under which the cost

function tends to $+\infty$ on the boundary of the set of positive-definite, Hermitian matrix, the minimum shrinkage factor for the existence of the CM estimator is obtained [36]. This result, however, can not directly determine the conditions of the two shrinkage factors affecting each other. In this work, we follow [36, Theorem 3] and its proof to study the RSKE. We first construct auxiliary functions by which the penalized negative log-likelihood function (4) can be lowerbounded. The two auxiliary functions have a similar form as (15) in [36]. Thus, using the same treatment of [36], we can examine the conditions for the auxiliary functions tending to $+\infty$ at the boundary. Based on the results, we can obtain the following sufficient condition for the existence of a solution to the RSKE:

Proposition 1: The cost function (4) has a finite lower bound over the set of positive-definite $\hat{\mathbf{R}}_A$ and $\hat{\mathbf{R}}_B$, i.e., a solution to (5) exists if the following conditions are satisfied:

- (1) None of $\mathbf{r}_{j,l}$ and $\mathbf{c}_{i,l}$ is an all-zero vector, where $\mathbf{r}_{j,l} \in \mathbb{C}^{N_A \times 1}$ denotes the j th row of \mathbf{Y}_l and $\mathbf{c}_{i,l} \in \mathbb{C}^{N_B \times 1}$ denotes the i th column of \mathbf{Y}_l ;
- (2) There exist $\beta_1 \in [0, 1], \beta_2 \in [0, 1]$ with $\beta_1 + \beta_2 = 1$ such that for any proper subspace $\mathcal{S}_A \subset \mathbb{C}^{N_A \times 1}$ and $\mathcal{S}_B \subset \mathbb{C}^{N_B \times 1}$ in the space of length- N_A and $-N_B$ vectors, respectively,

$$P_{LN_B}(\mathcal{S}_A) < \frac{(LN_B + \alpha_A L) \dim(\mathcal{S}_A) - \beta_2 LN}{\beta_1 LN}, \quad (7a)$$

$$P_{LN_A}(\mathcal{S}_B) < \frac{(LN_A + \alpha_B L) \dim(\mathcal{S}_B) - \beta_1 LN}{\beta_2 LN}, \quad (7b)$$

where $P_{LN_B}(\mathcal{S}_A) \triangleq \frac{\sum_{j=1}^{N_B} \sum_{l=1}^L 1_{\mathbf{r}_{j,l} \in \mathcal{S}_A}}{LN_B}$, $P_{LN_A}(\mathcal{S}_B) \triangleq \frac{\sum_{i=1}^{N_A} \sum_{l=1}^L 1_{\mathbf{c}_{i,l} \in \mathcal{S}_B}}{LN_A}$, 1_x denotes the indicator function.

Proof: See Appendix A.

In general, the above conditions require that the number of samples to be sufficiently large, and the samples are evenly spread out in the whole space.

Corollary 1: If the samples are evenly spread out in the whole space, such that $P_{LN_B}(\mathcal{S}_A) \leq \frac{\dim(\mathcal{S}_A)}{\min(N_A, LN_B)} = \frac{\dim(\mathcal{S}_A) \max(N_A, LN_B)}{LN}$ and $P_{LN_A}(\mathcal{S}_B) \leq \frac{\dim(\mathcal{S}_B) \max(N_B, LN_A)}{LN}$, then Condition (2) in Proposition 1 is equivalent to

$$\rho_A > 1 - \frac{LN_B}{\beta_1 \max(N_A, LN_B) + \beta_2 LN}, \quad (8a)$$

$$\rho_B > 1 - \frac{LN_A}{\beta_2 \max(N_B, LN_A) + \beta_1 LN}. \quad (8b)$$

Proof: Let $\dim(\mathcal{S}_A) \triangleq d_A$. Recall that $\alpha_A = \frac{N_B \rho_A}{1 - \rho_A}$ and $\alpha_B = \frac{N_A \rho_B}{1 - \rho_B}$. The condition (7a) is satisfied when

$$\frac{d_A \max(N_A, LN_B)}{LN} < \frac{\frac{LN_B d_A}{1 - \rho_A} - \beta_2 LN}{\beta_1 LN}. \quad (9)$$

Rearranging (9), one has $\rho_A > 1 - \frac{LN_B}{\beta_1 \max(N_A, LN_B) + \frac{\beta_2 LN}{d_A}}$ for arbitrary $d_A = 1, \dots, N_A - 1$, i.e.,

$$\begin{aligned} \rho_A &> \max_{d_A} \left(1 - \frac{LN_B}{\beta_1 \max(N_A, LN_B) + \frac{\beta_2 LN}{d_A}} \right) \\ &= 1 - \frac{LN_B}{\beta_1 \max(N_A, LN_B) + \beta_2 LN}, \end{aligned}$$

which is exactly (8a). Similarly, we have (8b).

Remark 1: Condition (2) in Corollary 1 shows the relationship between the shrinkage factors, the number of samples L , and the dimension of the sub-CMs N_A and N_B . In general, a larger shrinkage factor ρ_A is required when L decreases or N_A increases. Moreover, Condition (2) can be easily checked. For example, when $\beta_1 = 1$ and $\beta_2 = 0$, $\rho_A > \max(1 - \frac{LN_B}{\max(N_A, LN_B)}, 0)$ and $\rho_B > \max(1 - \frac{1}{N_B}, 0)$. When $N_B = 1$, $N = N_A$, the Kronecker structured CM reduces to an unstructured one. Then Condition (2) becomes $\rho_A > 1 - \frac{L}{\max(N, L)}$ and $\rho_B > 0$. When $L \geq N$, the condition is $\rho_A \in (0, 1)$. When $L < N$, the condition is $\rho_A \in (1 - \frac{L}{N}, 1)$, which agrees with the result in [35], [36] for the case of unstructured CM.

D. Iterative Solver and Its Convergence

Similarly to [34]–[37], we solve (5) by applying the process below, which involves two fixed-point iterations:

$$\hat{\mathbf{R}}_A^{(k+1)}(\rho_A) = (1 - \rho_A) \hat{\mathbf{C}}_A^{(k+1)} + \rho_A \mathbf{I}_{N_A}, \quad (10a)$$

$$\hat{\mathbf{R}}_B^{(k+1)}(\rho_B) = (1 - \rho_B) \hat{\mathbf{C}}_B^{(k+1)} + \rho_B \mathbf{I}_{N_B}, \quad (10b)$$

where

$$\hat{\mathbf{C}}_A^{(k+1)} = \frac{N_A}{L} \sum_{l=1}^L \frac{\mathbf{Y}_l^H (\hat{\mathbf{R}}_B^{(k)})^{-1} \mathbf{Y}_l}{\mathbf{y}_l^H (\hat{\mathbf{R}}_A^{(k)} \otimes \hat{\mathbf{R}}_B^{(k)})^{-1} \mathbf{y}_l}, \quad (11a)$$

$$\hat{\mathbf{C}}_B^{(k+1)} = \frac{N_B}{L} \sum_{l=1}^L \frac{\mathbf{Y}_l (\hat{\mathbf{R}}_A^{(k)})^{(-1)} \mathbf{Y}_l^H}{\mathbf{y}_l^H (\hat{\mathbf{R}}_A^{(k)} \otimes \hat{\mathbf{R}}_B^{(k)})^{-1} \mathbf{y}_l}, \quad (11b)$$

and $\hat{\mathbf{R}}_A^{(k)}$ and $\hat{\mathbf{R}}_B^{(k)}$ denote the estimates of the sub-CMs at the k th iteration. In this paper, we choose the initial CM estimates as $\hat{\mathbf{R}}_A^{(0)} = \mathbf{I}_{N_A}$ and $\hat{\mathbf{R}}_B^{(0)} = \mathbf{I}_{N_B}$ for simplicity.

It is useful to examine the convergence property of the above iterative estimator which generalizes Tyler's estimator [25] and its shrinkage extension [34], [36], [37] to the case of Kronecker-structured CM. The works [25], [34], [36], [37] assume unstructured CM and thus their solutions can be characterized by a single fixed-point equation. The convergence of the iterative process for Tyler's estimator is proved in [25] by examining the fixed-point iterations. For the shrinkage extension of Tyler's estimator, the convergence is proved in [34] by applying the concave Perron-Frobenius theory, in [36] by applying the majorization-minimization theorem, and in [37] by applying the monotone bounded convergence theorem. For the Kronecker-structured CM, though the case of the

KMLE has been studied in [41], in this work we incorporate shrinkage into the estimator and the convergence has not been analyzed earlier to the authors' best knowledge. Exploiting the majorization-minimization framework [72], we have the following proposition that establishes the converging property of the fixed-point iterations in (10).

Proposition 2: The fixed-point iterations in (10) converge to the solution of (5) for arbitrary positive-definite initial matrices $\hat{\mathbf{R}}_A^{(0)}$ and $\hat{\mathbf{R}}_B^{(0)}$ when the conditions in *Proposition 1* are satisfied.

Proof: See Appendix B.

Remark 2: The iterations in (10) can be terminated by using a distance metric

$$\mathcal{D}(\hat{\mathbf{R}}^{(k+1)}, \hat{\mathbf{R}}^{(k)}) = \left\| \frac{\hat{\mathbf{R}}^{(k+1)}}{\text{Tr}(\hat{\mathbf{R}}^{(k+1)})} - \frac{\hat{\mathbf{R}}^{(k)}}{\text{Tr}(\hat{\mathbf{R}}^{(k)})} \right\|, \quad (12)$$

where $\hat{\mathbf{R}}^{(k)} = \hat{\mathbf{R}}_A^{(k)} \otimes \hat{\mathbf{R}}_B^{(k)}$ and $\|\cdot\|$ denotes the Frobenius norm. This metric measures the variation of the solution over iterations. Then a stopping criterion can be set to terminate the iterations when

$$\mathcal{D}(\hat{\mathbf{R}}^{(k+1)}, \hat{\mathbf{R}}^{(k)}) < \delta \quad (13)$$

or $k > K_{\max}$ is met, where δ denotes a preset threshold and K_{\max} the maximum number of iterations allowed.

III. CHOICE OF THE SHRINKAGE FACTORS

The performance of the RSKE can be optimized by properly choosing the shrinkage factors ρ_A and ρ_B . In this section, we propose two different classes of choices, based on oracle approximating shrinkage (OAS) and leave-one-out cross validation (LOOCV), respectively, to provide solutions with different performance and complexity.

A. The KOAS Method

In [34], an OAS strategy for choosing the shrinkage factor for unstructured CM is derived by exploiting the MMSE criterion and plug-in estimates. We can extend this strategy to the RSKE. The choice of the two shrinkage factors will be decoupled into separate problems to enable a low-complexity solution. Following [34], we begin by assuming that the true CM \mathbf{R}_A and \mathbf{R}_B are already "known". Then, we choose to choose the shrinkage factors (ρ_A, ρ_B) that achieve the MMSE of the covariance matrix estimates as

$$\begin{aligned} \min_{\rho_A} \quad & \mathbb{E} \left\{ \left\| \hat{\mathbf{R}}_A - \mathbf{R}_A \right\|^2 \right\} \\ \text{s.t.} \quad & \hat{\mathbf{R}}_A = (1 - \rho_A) \mathbf{C}_A + \rho_A \mathbf{I}_{N_A}, \end{aligned} \quad (14)$$

and

$$\begin{aligned} \min_{\rho_B} \quad & \mathbb{E} \left\{ \left\| \hat{\mathbf{R}}_B - \mathbf{R}_B \right\|^2 \right\} \\ \text{s.t.} \quad & \hat{\mathbf{R}}_B = (1 - \rho_B) \mathbf{C}_B + \rho_B \mathbf{I}_{N_B}, \end{aligned} \quad (15)$$

where $\mathbb{E}\{\cdot\}$ denotes the mathematical expectation and

$$\begin{aligned} \mathbf{C}_A &\triangleq \frac{N}{LN_B} \sum_{l=1}^L \frac{\mathbf{Y}_l^H \mathbf{R}_B^{-1} \mathbf{Y}_l}{\mathbf{y}_l^H (\mathbf{R}_A \otimes \mathbf{R}_B)^{-1} \mathbf{y}_l}, \\ \mathbf{C}_B &\triangleq \frac{N}{LN_A} \sum_{l=1}^L \frac{\mathbf{Y}_l \mathbf{R}_A^{-1} \mathbf{Y}_l^H}{\mathbf{y}_l^H (\mathbf{R}_A \otimes \mathbf{R}_B)^{-1} \mathbf{y}_l}. \end{aligned} \quad (16)$$

The following proposition extends the OAS solution of [34] to the Kronecker-structured CM.

Proposition 3: The shrinkage factors that achieve the MMSE are given as

$$\rho_A^* = \frac{N_A^2 - \frac{1}{N_A} \text{Tr}(\mathbf{R}_A^2)}{(N_A^2 - N_A N_B L - L) + \left(N_B L + \frac{L-1}{N_A} \right) \text{Tr}(\mathbf{R}_A^2)}, \quad (17a)$$

$$\rho_B^* = \frac{N_B^2 - \frac{1}{N_B} \text{Tr}(\mathbf{R}_B^2)}{(N_B^2 - N_A N_B L - L) + \left(N_A L + \frac{L-1}{N_B} \right) \text{Tr}(\mathbf{R}_B^2)}. \quad (17b)$$

where we have used the assumption $\text{Tr}(\mathbf{R}_A) = N_A$ and $\text{Tr}(\mathbf{R}_B) = N_B$.

Proof: See Appendix C.

In practice, \mathbf{R}_A and \mathbf{R}_B in (17) are unknown. Similarly to [34], we propose to replace them by their trace-normalized estimates $\tilde{\mathbf{R}}_A$ and $\tilde{\mathbf{R}}_B$, such as the KNSCM [60] and KMLE [42]. We will show the performance of the resulting shrinkage factors $(\rho_{A,\text{KOAS}}, \rho_{B,\text{KOAS}})$, referred to as the Kronecker OAS (KOAS) choice, in Section IV. Note that, if $N_A = 1$ or $N_B = 1$, the Kronecker-structured CM reduces to the unstructured CM and (17) agrees with (17) in [34]. If $\rho_{A,\text{KOAS}} < 0$ is produced, we then truncate it to $\rho_{A,\text{KOAS}} = 0$. If $\rho_{A,\text{KOAS}} \geq 1$, we simply set the covariance matrix estimate to be the shrinkage target matrix. The treatments are similar for $\rho_{B,\text{KOAS}} < 0$ and $\rho_{B,\text{KOAS}} \geq 1$ and also the LOOCV-based choices of the shrinkage factors to be introduced in the next subsection.

B. The LOOCV Methods

We next provide alternative methods for choosing the shrinkage factors based on LOOCV. In order to achieve good performance and complexity tradeoff, the cost for LOOCV must be carefully chosen. In this work, we extend the quadratic cost used in [39] to obtain data-driven, analytical solutions. Note that [39] considers unstructured CM for Gaussian data, whereas this paper considers Kronecker structured CM estimation with elliptically distributed data for which iterative solvers are required. Two LOOCV solutions, i.e., CV-I and CV-II, will be introduced in this subsection.

1) *CV-I choice:* Let Σ_A and Σ_B be two positive-definite, Hermitian matrices. Define the following cost function

$$\mathcal{J}_A(\Sigma_A) = \mathbb{E} \left(\left\| \Sigma_A - \mathbf{S}_A \right\|^2 \right), \quad (18a)$$

$$\mathcal{J}_B(\Sigma_B) = \mathbb{E} \left(\left\| \Sigma_B - \mathbf{S}_B \right\|^2 \right), \quad (18b)$$

where the expectation is with respect to $\mathbf{Y} = \text{unvec}_{N_B N_A}(\mathbf{y})$,

$$\mathbf{S}_A \triangleq \frac{N_A \mathbf{Y}^H \mathbf{R}_B^{-1} \mathbf{Y}}{\mathbf{y}^H (\mathbf{R}_A \otimes \mathbf{R}_B)^{-1} \mathbf{y}}, \mathbf{S}_B \triangleq \frac{N_B \mathbf{Y} \mathbf{R}_A^{-1} \mathbf{Y}^H}{\mathbf{y}^H (\mathbf{R}_A^{-1} \otimes \mathbf{R}_B^{-1}) \mathbf{y}}. \quad (19)$$

Proposition 4: The expectation of \mathbf{S}_A and \mathbf{S}_B are respectively given as $\mathbb{E}(\mathbf{S}_A) = \mathbf{R}_A$ and $\mathbb{E}(\mathbf{S}_B) = \mathbf{R}_B$, and

$\mathcal{J}_A(\Sigma_A)$ and $\mathcal{J}_B(\Sigma_B)$ are minimized by $\Sigma_A = \mathbf{R}_A$ and $\Sigma_B = \mathbf{R}_B$, respectively.

Proof: See Appendix D.

Inspired by *Proposition 4*, we aim to estimate the cost function in (18) and then minimize it over the shrinkage factors. This may be achieved using different strategies, e.g., [31]. In this paper, we apply the LOOCV strategy [38] to estimate $\mathcal{J}_A(\Sigma_A)$ and $\mathcal{J}_B(\Sigma_B)$ and minimize them to determine the shrinkage factors. With the standard LOOCV, the samples \mathcal{Y} are repeatedly split into two sets. For the l th split, the samples in the training set \mathcal{Y}_l (with the l th sample \mathbf{y}_l omitted from \mathcal{Y}) are used for producing shrinkage CM estimates $\{\Sigma_A, \Sigma_B\}$ and the remaining sample \mathbf{y}_l is used for constructing $\{\mathbf{S}_A, \mathbf{S}_B\}$ to estimate $\mathcal{J}_A(\Sigma_A)$ and $\mathcal{J}_B(\Sigma_B)$. The standard LOOCV process requires the iterative estimator to be applied for L times for each pair of candidate shrinkage factors (ρ_A, ρ_B) , which can lead to significant complexity, especially when grid search of (ρ_A, ρ_B) is conducted. In order to address this complexity challenge, we propose alternative solutions by using proxy estimators so that closed-form expressions can be found for the optimized shrinkage factors.

Similarly to KOAS, we first assume that the covariance matrices are “known” and consider estimates of the covariance matrices from the samples $\mathcal{Y}_l = \{\mathbf{Y}_j, j \neq l\}$ as

$$\hat{\mathbf{R}}_A^{(l)}(\rho_A) = (1 - \rho_A)\hat{\mathbf{C}}_A^{(l)} + \rho_A \mathbf{I}_{N_A}, \quad (20a)$$

$$\hat{\mathbf{R}}_B^{(l)}(\rho_B) = (1 - \rho_B)\hat{\mathbf{C}}_B^{(l)} + \rho_B \mathbf{I}_{N_B}, \quad (20b)$$

where

$$\hat{\mathbf{C}}_A^{(l)} = \frac{N_A}{L-1} \sum_{j \neq l} \frac{\mathbf{Y}_j^H \mathbf{R}_B^{-1} \mathbf{Y}_j}{\mathbf{y}_j^H (\mathbf{R}_A \otimes \mathbf{R}_B)^{-1} \mathbf{y}_j}, \quad (21a)$$

$$\hat{\mathbf{C}}_B^{(l)} = \frac{N_B}{L-1} \sum_{j \neq l} \frac{\mathbf{Y}_j \mathbf{R}_A^{-1} \mathbf{Y}_j^H}{\mathbf{y}_j^H (\mathbf{R}_A \otimes \mathbf{R}_B)^{-1} \mathbf{y}_j}. \quad (21b)$$

Following [39], we adopt the quadratic cost functions below:

$$\mathcal{J}_{A,CV}(\hat{\mathbf{R}}_A) = \frac{1}{L} \sum_{l=1}^L \left\| \hat{\mathbf{R}}_A^{(l)}(\rho_A) - \hat{\mathbf{S}}_A^{(l)} \right\|^2, \quad (22a)$$

$$\mathcal{J}_{B,CV}(\hat{\mathbf{R}}_B) = \frac{1}{L} \sum_{l=1}^L \left\| \hat{\mathbf{R}}_B^{(l)}(\rho_B) - \hat{\mathbf{S}}_B^{(l)} \right\|^2, \quad (22b)$$

where

$$\hat{\mathbf{S}}_A^{(l)} = \frac{N_A \mathbf{Y}_l^H \mathbf{R}_B^{-1} \mathbf{Y}_l}{\mathbf{y}_l^H (\mathbf{R}_A \otimes \mathbf{R}_B)^{-1} \mathbf{y}_l}, \quad (23a)$$

$$\hat{\mathbf{S}}_B^{(l)} = \frac{N_B \mathbf{Y}_l \mathbf{R}_A^{-1} \mathbf{Y}_l^H}{\mathbf{y}_l^H (\mathbf{R}_A \otimes \mathbf{R}_B)^{-1} \mathbf{y}_l}. \quad (23b)$$

Substituting (20a) into (22a), the cost function can be rewritten as

$$\mathcal{J}_{A,CV}(\rho_A) = \frac{1}{L} \sum_{l=1}^L \left\| (1 - \rho_A)\hat{\mathbf{C}}_A^{(l)} + \rho_A \mathbf{I}_{N_A} - \hat{\mathbf{S}}_A^{(l)} \right\|^2. \quad (24)$$

We treat $\mathcal{J}_{A,CV}(\rho_A)$ as a proxy of $\mathcal{J}_A(\Sigma_A)$ and choose the shrinkage factor ρ_A as the minimizer of (24) as:

$$\rho_{A,CV} = \frac{\text{Re} \left(\sum_{l=1}^L \text{Tr} \left[\left(\mathbf{I}_{N_A} - \hat{\mathbf{C}}_A^{(l)} \right) \left(\hat{\mathbf{S}}_A^{(l)} - \hat{\mathbf{C}}_A^{(l)} \right) \right] \right)}{\sum_{l=1}^L \text{Tr} \left[\left(\mathbf{I}_{N_A} - \hat{\mathbf{C}}_A^{(l)} \right)^2 \right]}. \quad (25)$$

Similarly, we choose ρ_B as

$$\rho_{B,CV} = \frac{\text{Re} \left(\sum_{l=1}^L \text{Tr} \left[\left(\mathbf{I}_{N_B} - \hat{\mathbf{C}}_B^{(l)} \right) \left(\hat{\mathbf{S}}_B^{(l)} - \hat{\mathbf{C}}_B^{(l)} \right) \right] \right)}{\sum_{l=1}^L \text{Tr} \left[\left(\mathbf{I}_{N_B} - \hat{\mathbf{C}}_B^{(l)} \right)^2 \right]}. \quad (26)$$

Alternative expressions can be derived for (25) and (26) to reduce the computational costs. Let

$$\hat{\mathbf{C}}_A = \frac{N_A}{L} \sum_{l=1}^L \frac{\mathbf{Y}_l^H \mathbf{R}_B^{-1} \mathbf{Y}_l}{\mathbf{y}_l^H (\mathbf{R}_A \otimes \mathbf{R}_B)^{-1} \mathbf{y}_l}. \quad (27)$$

Recalling (21a) and (23a), we have

$$\hat{\mathbf{C}}_A^{(l)} = \frac{L}{L-1} \hat{\mathbf{C}}_A - \frac{1}{L-1} \hat{\mathbf{S}}_A^{(l)}, L \hat{\mathbf{C}}_A = \sum_{l=1}^L \hat{\mathbf{C}}_A^{(l)} = \sum_{l=1}^L \hat{\mathbf{S}}_A^{(l)}. \quad (28)$$

Note that $\hat{\mathbf{C}}_A$, $\hat{\mathbf{C}}_A^{(l)}$, $\hat{\mathbf{S}}_A^{(l)}$ and \mathbf{I}_{N_A} are all Hermitian matrices. By using (28), we have

$$\begin{aligned} \sum_{l=1}^L \text{Tr} \left(\hat{\mathbf{C}}_A^{(l)} \hat{\mathbf{S}}_A^{(l)} \right) &= \sum_{l=1}^L \text{Tr} \left(\left(\frac{L}{L-1} \hat{\mathbf{C}}_A - \frac{1}{L-1} \hat{\mathbf{S}}_A^{(l)} \right) \hat{\mathbf{S}}_A^{(l)} \right) \\ &= \frac{L^2}{L-1} \text{Tr} \left(\hat{\mathbf{C}}_A^2 \right) - \frac{\sum_{l=1}^L \text{Tr} \left(\left(\hat{\mathbf{S}}_A^{(l)} \right)^2 \right)}{L-1}, \end{aligned} \quad (29a)$$

$$\begin{aligned} \sum_{l=1}^L \text{Tr} \left(\left(\hat{\mathbf{C}}_A^{(l)} \right)^2 \right) &= \sum_{l=1}^L \text{Tr} \left(\left(\frac{L}{L-1} \hat{\mathbf{C}}_A - \frac{1}{L-1} \hat{\mathbf{S}}_A^{(l)} \right)^2 \right) \\ &= \frac{L^2(L-2)}{(L-1)^2} \text{Tr} \left(\hat{\mathbf{C}}_A^2 \right) + \frac{\sum_{l=1}^L \text{Tr} \left(\left(\hat{\mathbf{S}}_A^{(l)} \right)^2 \right)}{(L-1)^2}. \end{aligned} \quad (29b)$$

Substituting (29) into (25), we obtain (31a) on the next page to quickly evaluate the shrinkage factors $\rho_{A,CV-I}$. Similarly, we can obtain (31b) there for $\rho_{B,CV-I}$, where

$$\hat{\mathbf{C}}_B = \frac{N_B}{L} \sum_{l=1}^L \frac{\mathbf{Y}_l \mathbf{R}_A^{-1} \mathbf{Y}_l^H}{\mathbf{y}_l^H (\mathbf{R}_A \otimes \mathbf{R}_B)^{-1} \mathbf{y}_l}. \quad (30)$$

The shrinkage factors determined by (31) still require the true CM \mathbf{R}_A and \mathbf{R}_B to be known to compute (27), (30), and (23). Similarly to KOAS, we propose to substitute them by their trace-normalized estimates $\hat{\mathbf{R}}_A$ and $\hat{\mathbf{R}}_B$. We refer to the resultant solutions as the CV-I choice.

$$\rho_{A,CV-I} = \frac{-\frac{L}{(L-1)^2} \text{Tr}(\hat{\mathbf{C}}_A^2) + \frac{1}{(L-1)^2} \sum_{l=1}^L \text{Tr}((\hat{\mathbf{S}}_A^{(l)})^2)}{N_A - 2\text{Tr}(\hat{\mathbf{C}}_A) + \frac{L(L-2)}{(L-1)^2} \text{Tr}(\hat{\mathbf{C}}_A^2) + \frac{1}{L(L-1)^2} \sum_{l=1}^L \text{Tr}((\hat{\mathbf{S}}_A^{(l)})^2)}. \quad (31a)$$

$$\rho_{B,CV-I} = \frac{-\frac{L}{(L-1)^2} \text{Tr}(\hat{\mathbf{C}}_B^2) + \frac{1}{(L-1)^2} \sum_{l=1}^L \text{Tr}((\hat{\mathbf{S}}_B^{(l)})^2)}{N_B - 2\text{Tr}(\hat{\mathbf{C}}_B) + \frac{L(L-2)}{(L-1)^2} \text{Tr}(\hat{\mathbf{C}}_B^2) + \frac{1}{L(L-1)^2} \sum_{l=1}^L \text{Tr}((\hat{\mathbf{S}}_B^{(l)})^2)}. \quad (31b)$$

2) *CV-II choice*: As shown later in the simulation, the performance of KOAS and CV-I depend on the choice of the plug-in estimates $\tilde{\mathbf{R}}_A$ and $\tilde{\mathbf{R}}_B$. In order to address this challenge, we propose to choose $\tilde{\mathbf{R}}_A$ and $\tilde{\mathbf{R}}_B$ used in the CV-I method as the current CM estimates at each iteration, i.e., $\hat{\mathbf{R}}_A^{(k)}$ and $\hat{\mathbf{R}}_B^{(k)}$, and refer to the resulting solutions as the CV-II choice. Specifically, at the k th iteration, the CMs estimated from the l -th training subset of LOOCV are constructed as

$$\hat{\mathbf{R}}_A^{(k+1,l)}(\rho_A) = (1 - \rho_A)\hat{\mathbf{C}}_A^{(k+1,l)} + \rho_A \mathbf{I}_{N_A}, \quad (32a)$$

$$\hat{\mathbf{R}}_B^{(k+1,l)}(\rho_B) = (1 - \rho_B)\hat{\mathbf{C}}_B^{(k+1,l)} + \rho_B \mathbf{I}_{N_B}, \quad (32b)$$

where

$$\hat{\mathbf{C}}_A^{(k+1,l)} = \frac{N_A}{L-1} \sum_{j \neq l} \frac{\mathbf{Y}_j^H (\hat{\mathbf{R}}_B^{(k)})^{-1} \mathbf{Y}_j}{\mathbf{y}_j^H (\hat{\mathbf{R}}_A^{(k)} \otimes \hat{\mathbf{R}}_B^{(k)})^{-1} \mathbf{y}_j}, \quad (33a)$$

$$\hat{\mathbf{C}}_B^{(k+1,l)} = \frac{N_B}{L-1} \sum_{j \neq l} \frac{\mathbf{Y}_j (\hat{\mathbf{R}}_A^{(k)})^{(-1)} \mathbf{Y}_j^H}{\mathbf{y}_j^H (\hat{\mathbf{R}}_A^{(k)} \otimes \hat{\mathbf{R}}_B^{(k)})^{-1} \mathbf{y}_j}, \quad (33b)$$

where $\hat{\mathbf{R}}_A^{(k)}$ and $\hat{\mathbf{R}}_B^{(k)}$ are the CM estimates from the previous iteration, which are always positive-definite if the shrinkage factors are non-zero.

Similarly to the CV-I choice, we then adopt the following LOOCV cost functions

$$\mathcal{J}_{A,CV}^{(k+1)}(\hat{\mathbf{R}}_A) = \frac{1}{L} \sum_{l=1}^L \left\| \hat{\mathbf{R}}_A^{(k+1,l)}(\rho_A) - \hat{\mathbf{S}}_A^{(k+1,l)} \right\|^2, \quad (34a)$$

$$\mathcal{J}_{B,CV}^{(k+1)}(\hat{\mathbf{R}}_B) = \frac{1}{L} \sum_{l=1}^L \left\| \hat{\mathbf{R}}_B^{(k+1,l)}(\rho_B) - \hat{\mathbf{S}}_B^{(k+1,l)} \right\|^2, \quad (34b)$$

where

$$\hat{\mathbf{S}}_A^{(k+1,l)} = \frac{N_A \mathbf{Y}_l^H (\hat{\mathbf{R}}_B^{(k)})^{-1} \mathbf{Y}_l}{\mathbf{y}_l^H (\hat{\mathbf{R}}_A^{(k)} \otimes \hat{\mathbf{R}}_B^{(k)})^{-1} \mathbf{y}_l}, \quad (35a)$$

$$\hat{\mathbf{S}}_B^{(k+1,l)} = \frac{N_B \mathbf{Y}_l (\hat{\mathbf{R}}_A^{(k)})^{(-1)} \mathbf{Y}_l^H}{\mathbf{y}_l^H (\hat{\mathbf{R}}_A^{(k)} \otimes \hat{\mathbf{R}}_B^{(k)})^{-1} \mathbf{y}_l}. \quad (35b)$$

The CV-II choice of the shrinkage factors are then given as the minimizers of (34a) and (34b) and their analytical expressions are given by (36) on the following page. As such, the shrinkage factors in (10) are updated at each iteration as $\rho_{A,CV-II}^{(k+1)}$ and $\rho_{B,CV-II}^{(k+1)}$.

C. Remarks

Remark 3: The proposed methods exhibit different complexities. If the shrinkage factors are given, the computational complexity of the iterative process in (10) is about $\mathcal{O}(N_{it}(N_A^3 + N_B^3 + L(N_A N_B^2 + N_A^2 N_B)))$, where N_{it} denotes the number of iterations, and we have used the identities $(\mathbf{A} \otimes \mathbf{B})^{-1} = \mathbf{A}^{-1} \otimes \mathbf{B}^{-1}$ and $(\mathbf{B}^T \otimes \mathbf{A})\text{vec}(\mathbf{X}) = \text{vec}(\mathbf{A}\mathbf{X}\mathbf{B})$. All the shrinkage factors proposed are given in closed forms without the need of grid search. Their complexities are summarized below, where only the highest order of the complexity is counted.

- **KOAS**: The computational complexity of (17) mainly arises from the computation of $\text{Tr}(\hat{\mathbf{R}}_A^2)$ and $\text{Tr}(\hat{\mathbf{R}}_B^2)$, which is $\mathcal{O}(N_A^2 + N_B^2)$ when the plug-in CMs $\tilde{\mathbf{R}}_A$ and $\tilde{\mathbf{R}}_B$ are known.
- **CV-I**: Given $\tilde{\mathbf{R}}_A$ and $\tilde{\mathbf{R}}_B$, (31) can be evaluated at a complexity of $\mathcal{O}(N_A^3 + N_B^3 + L(N_A^2 N_B + N_A N_B^2))$.
- **CV-II**: Note that (36) has a similar form as (31). Furthermore, (36) can be evaluated by reusing the intermediate results, such as $\hat{\mathbf{C}}_A^{(k+1)}$ and $\hat{\mathbf{C}}_B^{(k+1)}$, for updating the CM in the iterative process in (10). As such, computing the shrinkage factors costs $\mathcal{O}(N_{it}L(N_A^2 + N_B^2))$. Note that the CV-II choice does not require extra plug-in CM estimates.

It can be seen that, ignoring the cost for finding the plug-in CMs, the complexity of finding the shrinkage factors is dominated by that of iteratively updating the CMs in (10). In contrast to CV-II, both KOAS and CV-I require extra cost for finding the plug-in CMs. For example, finding the KNSCM and KMLE requires complexity of $\mathcal{O}(L(N_A N_B^2 + N_A^2 N_B))$ and $\mathcal{O}(N_{it}'(N_A^3 + N_B^3 + L(N_A N_B^2 + N_A^2 N_B)))$, respectively, where N_{it}' is the number of iterations for KMLE. In particular, the KMLE has the same order of complexity as the RSKE.

Remark 4: The CV-II choice iteratively updates the shrinkage factors by treating the current estimates of the CMs $\hat{\mathbf{R}}_A^{(k)}$ and $\hat{\mathbf{R}}_B^{(k)}$ as constant which are independent of the samples. The LOOCV applied to choose ρ_A at iteration k can be regarded as a procedure to locally optimize the shrinkage

$$\rho_{A,CV-II}^{(k+1)} = \frac{-\frac{L}{(L-1)^2} \text{Tr} \left(\left(\hat{\mathbf{C}}_A^{(k+1)} \right)^2 \right) + \frac{1}{(L-1)^2} \sum_{l=1}^L \text{Tr} \left(\left(\hat{\mathbf{S}}_A^{(k+1,l)} \right)^2 \right)}{N_A - 2\text{Tr} \left(\hat{\mathbf{C}}_A^{(k+1)} \right) + \frac{L(L-2)}{(L-1)^2} \text{Tr} \left[\left(\hat{\mathbf{C}}_A^{(k+1)} \right)^2 \right] + \frac{1}{L(L-1)^2} \sum_{l=1}^L \text{Tr} \left[\left(\hat{\mathbf{S}}_A^{(k+1,l)} \right)^2 \right]}. \quad (36a)$$

$$\rho_{B,CV-II}^{(k+1)} = \frac{-\frac{L}{(L-1)^2} \text{Tr} \left(\left(\hat{\mathbf{C}}_B^{(k+1)} \right)^2 \right) + \frac{1}{(L-1)^2} \sum_{l=1}^L \text{Tr} \left(\left(\hat{\mathbf{S}}_B^{(k+1,l)} \right)^2 \right)}{N_B - 2\text{Tr} \left(\hat{\mathbf{C}}_B^{(k+1)} \right) + \frac{L(L-2)}{(L-1)^2} \text{Tr} \left[\left(\hat{\mathbf{C}}_B^{(k+1)} \right)^2 \right] + \frac{1}{L(L-1)^2} \sum_{l=1}^L \text{Tr} \left[\left(\hat{\mathbf{S}}_B^{(k+1,l)} \right)^2 \right]}. \quad (36b)$$

estimation of the covariance matrix \mathbf{R}_A using the rows of $\{\mathbf{Y}_l\}$ after being normalized by $\sqrt{\mathbf{y}_j^H \left(\hat{\mathbf{R}}_A^{(k)} \otimes \hat{\mathbf{R}}_B^{(k)} \right)^{-1} \mathbf{y}_j}$ and decorrelated using $\hat{\mathbf{R}}_B^{(k)}$.

Remark 5: The KOAS and CV-I choices produce (ρ_A, ρ_B) that are fixed during the iterative process. The convergence of the iterative solver for this case has been proved in Section II-D. However, the performance can be affected by the prior estimates used. By contrast, the CV-II choice adapts (ρ_A, ρ_B) during the iterations and works for arbitrary positive-definite, Hermitian initial estimates. This results in the cost function in (4) and the fixed-point iterations in (5) change over iterations. Proofs of the existence of an solution and the convergence of the iterative algorithm are unavailable for the CV-II choice. However, numerical studies show that the CV-II choice still leads to converging solutions and better performance compared with the CV-I choice in cases with very low sample supports.

IV. APPLICATION TO PSTAP

In this section, we consider an application of the proposed estimator to PSTAP. Following [60], consider a pulsed Doppler radar deploying a uniform linear array (ULA) of N_s antennas, each of which can measure electromagnetic wave in N_p polarization channels [55], [73]. A burst of N_t identical pulses at a constant pulse repetition frequency (PRF) of f_r are transmitted during the coherent processing interval (CPI). The received signals of all the polarization channels at each sensor in the cell under test (CUT) are down-converted to baseband or to an intermediate frequency in all the pulses at each sensor. They are then processed by the corresponding matched filters and sampled and stacked into an N -dimensional vector $\mathbf{y} \in \mathbb{C}^{N \times 1}$, where $N = N_p N_t N_s$. Let $\mathbf{y}_l, l = 1, 2, \dots, L$ be L independent, identically distributed (i.i.d) signal-free secondary data, arising from adjacent range cells.

Radar detection is a binary hypothesis testing problem, where hypotheses H_0 and H_1 correspond to target absence and presence, respectively. We first ignore noise in the received signal, which approximates the case of high clutter-to-noise-ratio (CNR). The received signal can then be approximately modeled as [60], [74]

$$\begin{cases} H_0 : & \mathbf{y} = \mathbf{c}_0 \\ & \mathbf{y}_l = \mathbf{c}_l, l = 1, 2, \dots, L \\ H_1 : & \mathbf{y} = \alpha \mathbf{s} + \mathbf{c}_0 \\ & \mathbf{y}_l = \mathbf{c}_l, l = 1, 2, \dots, L \end{cases} \quad (37)$$

where α denotes the complex amplitude of the target signal, \mathbf{s} denotes the steering vector of target, $\{\mathbf{c}_l\}$ denote the clutter returns in the CUT and adjacent cells. In many radar scenarios, experimental trials have shown a good fitting of the compound Gaussian model to the heterogeneous clutter measurements [12], [14]. The received clutter can then be modeled as the product of a positive texture τ and a Gaussian vector referred to as speckle \mathbf{u} , i.e.,

$$\begin{cases} \mathbf{c}_0 = \sqrt{\tau_0} \mathbf{u}_0 \in \mathbb{C}^{N \times 1}, \\ \mathbf{c}_l = \sqrt{\tau_l} \mathbf{u}_l \in \mathbb{C}^{N \times 1}, \end{cases} \quad (38)$$

where τ_l is the texture and \mathbf{u}_l the speckle component. We assume $\mathbb{E}(\tau_l) < \infty, \forall l$, so that the CM of \mathbf{c}_l exists, where $\mathbb{E}(\cdot)$ denotes the mathematical expectation. We assume that all the clutter patches are associated with the same terrain and thus \mathbf{u}_l are i.i.d with a shared covariance matrix \mathbf{R} . For conciseness, we here drop the subscript l of \mathbf{u}_l while discussing its covariance matrix \mathbf{R} below. Assume that an estimate $\hat{\mathbf{R}}$ of \mathbf{R} is known, then a receiving filter

$$\mathbf{w} = \frac{\hat{\mathbf{R}}^{-1} \mathbf{s}}{\mathbf{s}^H \hat{\mathbf{R}}^{-1} \mathbf{s}} \quad (39)$$

can be applied to suppress the clutter in the observation \mathbf{y} to facilitate the detection, where $(\cdot)^H$ denotes conjugate transpose. Clearly, it is desired to obtain an accurate and well-conditioned estimate $\hat{\mathbf{R}}$.

Similarly to the conventional STAP system [66], the clutter signal for a polarimetric radar can be expressed as the sum of N_c clutter patches in the same range cell, i.e.,

$$\mathbf{u} = \sum_{i=1}^{N_c} \mathbf{a}_c^{(i)} \otimes \mathbf{p}_c^{(i)} \in \mathbb{C}^{N \times 1}, \quad (40)$$

where $\mathbf{a}_c^{(i)} \in \mathbb{C}^{N_s N_t \times 1}$ and $\mathbf{p}_c^{(i)} \in \mathbb{C}^{N_p \times 1}$ denote the space-time steering vector and polarization scattering vector of the i th clutter patch, respectively. Similarly, the polarization-space-time steering vector of the target can be written as $\mathbf{s} = \mathbf{a}_t \otimes \mathbf{p}_t$, where \mathbf{a}_t denotes the target space-time steering vector which depends on the direction and velocity of the target.

Following [75], we assume that $N_p = 3$ and $\mathbf{p}_c^{(i)}$ consists of three complex elements: HH, VV, and HV, i.e.,

$$\mathbf{p}_c^{(i)} = \begin{bmatrix} p_{c,hh}^{(i)} & p_{c,vv}^{(i)} & p_{c,hv}^{(i)} \end{bmatrix}^T, \quad (41)$$

where $(\cdot)^T$ denotes the transpose. Furthermore, we assume $\mathbf{p}_c^{(i)}$ follows a complex Gaussian distribution with zero mean and covariance matrix [60], [75]

$$\mathbb{E} \left(\mathbf{p}_c^{(i)} \left(\mathbf{p}_c^{(i)} \right)^H \right) = \varepsilon_i \begin{bmatrix} 1 & \rho_c \sqrt{\gamma_c} & 0 \\ (\rho_c)^* \sqrt{\gamma_c} & \gamma_c & 0 \\ 0 & 0 & \delta_c \end{bmatrix}, \quad (42)$$

with

$$\begin{aligned} \varepsilon_i &= \mathbb{E} \left(\left| p_{c,hh}^{(i)} \right|^2 \right), & \delta_c &= \frac{\mathbb{E} \left(\left| p_{c,hv}^{(i)} \right|^2 \right)}{\mathbb{E} \left(\left| p_{c,hh}^{(i)} \right|^2 \right)}, \\ \gamma_c &= \frac{\mathbb{E} \left(\left| p_{c,vv}^{(i)} \right|^2 \right)}{\mathbb{E} \left(\left| p_{c,hh}^{(i)} \right|^2 \right)}, & \rho_c &= \frac{\mathbb{E} \left(p_{c,hh}^{(i)} \left(p_{c,vv}^{(i)} \right)^* \right)}{\left[\mathbb{E} \left(\left| p_{c,hh}^{(i)} \right|^2 \right) \mathbb{E} \left(\left| p_{c,vv}^{(i)} \right|^2 \right) \right]^{1/2}}, \end{aligned} \quad (43)$$

where $(\cdot)^*$ denotes conjugate.

The space-time steering vector is expressed as

$$\mathbf{a}_c^{(i)} = \mathbf{a}_d(f_{d,i}) \otimes \mathbf{a}_s(f_{s,i}) \in \mathbb{C}^{N_s N_t \times 1}, \quad (44)$$

where $f_{d,i} = (2v_a/\lambda f_r) \cos(\phi_i)$ denotes the normalized Doppler frequency, $f_{s,i} = (d/\lambda) \cos(\phi_i)$ the normalized spatial frequency, d the inter-element spacing, v_a the velocity of the platform, λ the radar wavelength, ϕ_i the direction of i th clutter patch with respect to the array, \otimes the Kronecker product, and

$$\begin{aligned} \mathbf{a}_d(f_{d,i}) &= \left[1, e^{j2\pi f_{d,i}}, \dots, e^{j2\pi(N_t-1)f_{d,i}} \right]^T \in \mathbb{C}^{N_t \times 1}, \\ \mathbf{a}_s(f_{s,i}) &= \left[1, e^{j2\pi f_{s,i}}, \dots, e^{j2\pi(N_s-1)f_{s,i}} \right]^T \in \mathbb{C}^{N_s \times 1}, \end{aligned} \quad (45)$$

are the temporal and spatial steering vectors, respectively.

The covariance matrix of \mathbf{u} can be given as [60]

$$\mathbf{R} = \mathbb{E}(\mathbf{u}\mathbf{u}^H) = \mathbf{R}_{st} \otimes \mathbf{R}_p \in \mathbb{C}^{N \times N}, \quad (46)$$

where the space-time and polarization covariance matrices are respectively defined as

$$\mathbf{R}_{st} \triangleq \sum_{i=1}^{N_c} \varepsilon_i \alpha_c^{(i)} \left(\alpha_c^{(i)} \right)^H \in \mathbb{C}^{N_s N_t \times N_s N_t}, \quad (47)$$

and

$$\mathbf{R}_p \triangleq \begin{bmatrix} 1 & \rho_c \sqrt{\gamma_c} & 0 \\ (\rho_c)^* \sqrt{\gamma_c} & \gamma_c & 0 \\ 0 & 0 & \delta_c \end{bmatrix} \in \mathbb{C}^{3 \times 3}. \quad (48)$$

The above analysis suggests that, with unknown π_l , the clutter observations in (37), i.e., $\mathbf{y}_l, l = 1, 2, \dots, L$, follow a compound Gaussian distribution sharing the Kronecker-structured covariance matrix \mathbf{R} of the speckle \mathbf{u}_l . The RSKE techniques discussed above can be applied to obtain $\hat{\mathbf{R}}$ required in (39) from the training samples $\mathbf{y}_l, l = 1, 2, \dots, L$. Note that if $N_p = 1$, the above PSTAP scenario becomes the conventional STAP case.

In practice, noise exists in the observations, i.e., the signal for the CUT is modeled as

$$\begin{cases} H_0: & \mathbf{y} = \mathbf{c}_0 + \mathbf{n}_0 = \sqrt{\tau_0} \mathbf{u}_0 + \mathbf{n}_0 \\ H_1: & \mathbf{y} = \alpha \mathbf{s} + \mathbf{c}_0 + \mathbf{n}_0 = \alpha \mathbf{s} + \sqrt{\tau_0} \mathbf{u}_0 + \mathbf{n}_0 \end{cases} \quad (49)$$

while the signals for the adjacent cells follow

$$\mathbf{y}_l = \mathbf{c}_l + \mathbf{n}_l = \sqrt{\tau_l} \mathbf{u}_l + \mathbf{n}_l, \quad l = 1, 2, \dots, L, \quad (50)$$

where $\mathbf{n}_l \sim \mathcal{CN}(\mathbf{0}, \sigma^2 \mathbf{I}_N)$ is the additive white Gaussian noise (AWGN) and \mathbf{u}_l follows (40). Strictly speaking, the secondary data (50) deviates from the compound Gaussian model due to the additional Gaussian components \mathbf{n}_l , even though the power of the clutter is always assumed to be much stronger than that of the noise [76], [77]. We study in Section V-B the performance of the RSKE with such model mismatch to show its practical value. With τ_0 given, the true covariance matrix of the clutter-plus-noise in the CUT is given by

$$\mathbf{R}_0 = \tau_0 \mathbf{R} + \sigma^2 \mathbf{I}.$$

In this case, the output signal-to-clutter-noise ratio (SCNR) using the receiver filter (39) is evaluated as

$$\text{SCNR} = \frac{|\alpha|^2 (\mathbf{s}^H \hat{\mathbf{R}}^{-1} \mathbf{s})^2}{\mathbf{s}^H \hat{\mathbf{R}}^{-1} \mathbf{R}_0 \hat{\mathbf{R}}^{-1} \mathbf{s}}$$

which is upper bounded by SCNR achieved with $\hat{\mathbf{R}} = \mathbf{R}_0$:

$$\text{SCNR}^* = |\alpha|^2 |\mathbf{s}^H \mathbf{R}_0^{-1} \mathbf{s}|.$$

It is common to evaluate the performance using the normalized SCNR loss [3], [68], [69]

$$\text{SCNR}_{\text{loss}} = \frac{\text{SCNR}}{\text{SCNR}^*} = \frac{(\mathbf{s}^H \hat{\mathbf{R}}^{-1} \mathbf{s})^2}{(\mathbf{s}^H \hat{\mathbf{R}}^{-1} \mathbf{R}_0 \hat{\mathbf{R}}^{-1} \mathbf{s}) (\mathbf{s}^H \mathbf{R}_0^{-1} \mathbf{s})}. \quad (51)$$

Clearly its maximum $\text{SCNR}_{\text{loss}} = 1$ is achieved when the covariance matrix is perfectly estimated and a larger value indicates better performance.

V. SIMULATION RESULTS

In this section, we show the performance of the proposed RSKE estimators. We compare the proposed estimators with the following CM estimators: SCM [78], KMLE [42], [60], and KNSCM [60]. For the RSKE, in addition to the KOAS and CV choices of the shrinkage factors, the oracle choice of the shrinkage factors is also considered, which minimizes the NMSE defined in (52) at each iteration under the assumption that the true CM is known.

A. CM Estimation Accuracy

In order to evaluate the CM estimation accuracy, we use the following normalized mean-square error (NMSE) as the performance metric [79]:

$$\text{NMSE} \triangleq \frac{\mathbb{E} \left\{ \left\| \hat{\mathbf{R}} / \text{Tr}(\hat{\mathbf{R}}) - \mathbf{R} / \text{Tr}(\mathbf{R}) \right\|^2 \right\}}{\left\| \mathbf{R} / \text{Tr}(\mathbf{R}) \right\|^2}. \quad (52)$$

Consider an example with the autoregressive (AR) covariance matrices, whose (i, j) th entries are given as

$$\begin{aligned} [\mathbf{R}_A]_{i_A, j_A} &= \epsilon_A^{|i_A - j_A|}, \quad 1 \leq i_A, j_A \leq N_A, \\ [\mathbf{R}_B]_{i_B, j_B} &= \epsilon_B^{|i_B - j_B|}, \quad 1 \leq i_B, j_B \leq N_B, \end{aligned} \quad (53)$$

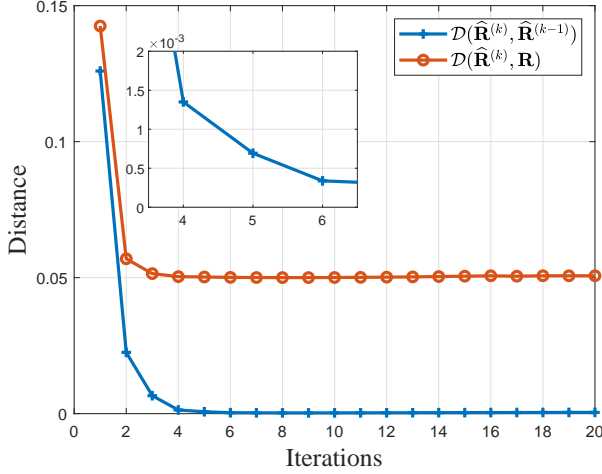


Fig. 1: $\mathcal{D}(\hat{\mathbf{R}}^{(k)}, \hat{\mathbf{R}}^{(k-1)})$ over iterations for RSKE with CV-II.

which has been widely considered for evaluating CM estimation techniques [34], [39], [60]. Here we first set $N_A = 6$, $N_B = 6$, $\epsilon_A = 0.1$ and $\epsilon_B = 0.9$. Then the samples are generated according to $\mathbf{y}_l = \sqrt{\tau_l} \mathbf{u}_l$, $l = 1, 2, \dots, L$, where the texture τ_l follows a Gamma distribution [75] of shape parameter ν and scale parameter $1/\nu$, i.e., $\tau_l \sim \Gamma(\nu, 1/\nu)$, $\mathbf{u}_l \sim \mathcal{CN}(\mathbf{0}, \mathbf{R})$. The generated samples $\{\mathbf{y}_l\}$ follow a zero-mean CES distribution. The estimated sub-CMs $\hat{\mathbf{R}}_A^{(k)}$ and $\hat{\mathbf{R}}_B^{(k)}$ in (11) are initialized as identity matrices for simplicity but other initializations can produce similar results.

As CV-II leads to shrinkage factors varying over iterations and a proof of the convergence of the resulting RSKE is unavailable, we resort to numerical studies. 200 Monte-Carlo experiments are performed. Fig. 1 shows the average of $\mathcal{D}(\hat{\mathbf{R}}^{(k)}, \hat{\mathbf{R}}^{(k-1)})$ varying with the iterations where CV-II is applied. We can see that $\hat{\mathbf{R}}_A$ and $\hat{\mathbf{R}}_B$ of CV-II tend to stabilize over iterations. This indicates that CV-II also leads to converging solutions. The distance between $\hat{\mathbf{R}}^{(k)}$ and \mathbf{R} also decreases over iterations, indicating improved accuracy of the CM estimate over iterations. Furthermore, a small number of iterations is sufficient for approaching the performance limit of the RSKE. In the rest of this section, for terminating the iterations, we choose the threshold δ in (13) as 10^{-3} and $K_{\max} = 15$.

Fig. 2 shows the NMSE performance under different numbers of samples L . For each abscissa, 2000 Monte-Carlo experiments are performed. We can see that the proposed RSKE can improve the estimation accuracy as compared with several existing estimators in different cases. The CV choices of the shrinkage factors can produce near-oracle performance. The performance with KOAS and CV-I depends on the choice of the plug-in estimates used. In contrast, CV-II, which does not require plug-in estimates, performs the best.

Fig. 3 shows the NMSE versus ρ_A and ρ_B , where we set $N_A = 8$, $N_B = 8$, $\epsilon_A = 0.3$, $\epsilon_B = 0.7$ and $L = 10$. 100 Monte-Carlo experiments are performed. The average NMSE achieved by RSKE with different ρ_A and ρ_B is demonstrated in Fig. 3 where the averages of the shrinkage factors chosen

TABLE I: Radar parameters

Carrier frequency f_0	1.2 GHz
Wavelength λ_0	0.25 m
PRF f_r	2000Hz
Platform velocity v	125 m/s
Platform altitude	3000 m
Bandwidth	12 MHz
Sampling frequency	20 MHz

by KOAS and CV-I are also marked. It confirms that the different plug-in estimators used lead to different shrinkage factors. Moreover, CV-I yields solutions closer to the oracle ones compared to KOAS.

Fig. 4 shows the NMSE performance versus dimension N . As $N = N_A N_B$, we fix $N_B = 4$ and vary N_A . We set $\epsilon_A = 0.1$, $\epsilon_B = 0.9$ and $\nu = 10$. For each abscissa, 2000 Monte-Carlo experiments are performed. The plug-in CM estimate for both KOAS and CV-I are chosen as the KNSCM for its simplicity. The number of training samples is set as $L = N/4$, which increases with N_A (and also N). From Fig. 4, we can see that the NMSE of the proposed estimators approaches that of the oracle estimator as N_A (and N) increases.

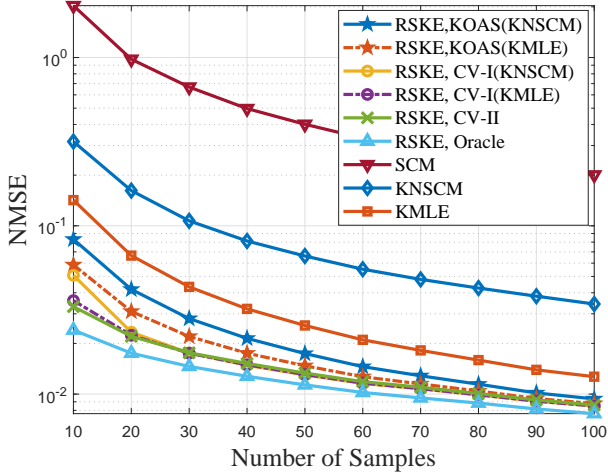
Fig. 5 shows the condition number of the estimated CM of RSKE (with CV-I, CV-II, KOAS), KMLE and KNSCM. Here we set $N_A = 8$, $N_B = 8$, $\epsilon_A = 0.1$ and $\epsilon_B = 0.9$. We set the plug-in estimator for CV-I and KOAS as KNSCM. One can see that the proposed CV-I, CV-II and KOAS algorithms yield CM estimates which are better-conditioned than those with KNSCM and KMLE, especially when the number of samples is small. As they also improve the NMSE, it is expected that the RSKE with the proposed shrinkage factor choices can improve the performance for applications where the inverse of the CM is required, such as beamforming and spectral estimation applications.

B. Clutter Suppression Performance in PSTAP

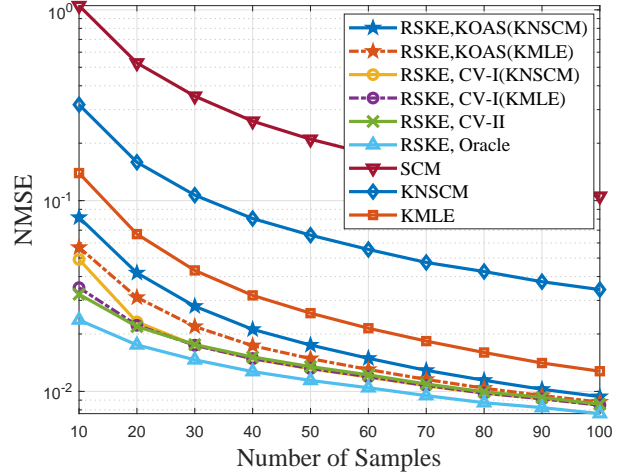
In this section, we show simulation results to demonstrate the performance of the RSKE for the application of PSTAP as introduced in Section IV. In our simulations, the samples are generated according to (49) and (50). The texture $\tau_l \sim \Gamma(1, 1)$. The number of elements $N_s = 4$ and the number of pulses $N_t = 4$. Hence, the total dimension N is 48 here and the abscissa is set from 16 to 128 with the step 16. The interelement spacing of the ULA is $d = \lambda_0/2$, where λ_0 denotes the wavelength. Each clutter ring is divided into 401 clutter patches. Other radar parameters are listed in Table I. Note that the CNR is computed as

$$\text{CNR} = \frac{\mathbb{E}[||\mathbf{u}||^2]}{N\sigma^2}.$$

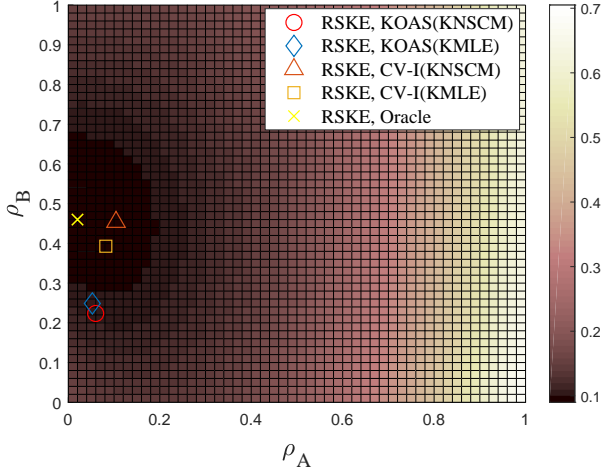
Here we set $\text{CNR} = 20$ dB, the normalized Doppler frequency of the target as 0.4 and its azimuth and elevation angle as 0° and 3.6° , respectively. The scattering feature of the target is set $\mathbf{p}_t = [2j, 1j, 0.5]^T$ here. We set $\rho_c = 1.3$, $\gamma_c = 0.1$ and $\delta_c = 0.9$ for \mathbf{R}_p in (48). We use the SCNR loss (51) to demonstrate the performance of the CM estimation



(a)



(b)

Fig. 2: NMSE versus the number of samples L . (a) $\nu = 1$; (b) $\nu = 10$;Fig. 3: NMSE versus ρ_A and ρ_B .

in suppressing the clutter. Recalling (51), we can see that $\text{SCNR}_{\text{loss}}$ is irrelevant to α . Without loss of generality, we fix $\alpha = 1$ in (49).

Fig. 6 shows the performance for the PSTAP application versus the sample number L . For each abscissa, 1000 Monte-Carlo experiments are performed. It is seen that the proposed methods can achieve the best clutter suppression performance among several estimators under different amount of training data. This shows that the RSKE is effective for the PSTAP application, even the clutter-plus-noise involved is a mixture of CES data and Gaussian data.

VI. CONCLUSIONS

In this paper, we investigate a robust, iterative shrinkage estimator, which is referred to as RSKE, for estimating the CM with the Kronecker product structure. The RSKE can be obtained by minimizing a negative log-likelihood function penalized by Kullback-Leibler divergence and interpreted by

integrating linear shrinkage into the fixed-point iterations. The conditions for the existence of the RSKE are investigated and the convergence of the iterative solver is investigated. We also introduce three methods for choosing the shrinkage factors by exploiting oracle approximating shrinkage (OAS) and cross-validation (CV), respectively. The proposed estimators are then applied to PSTAP in the heterogeneous context. Compared with the state-of-the-art estimators, the RSKE achieves more accurate CM estimation and improves the condition number by significantly reducing the number of unknown parameters and integrating shrinkage into the robust estimation.

APPENDIX A PROOF OF PROPOSITION 1

In this appendix, we examine the conditions under which a solution to (5) exists by constructing two auxiliary functions to lowerbound the cost function in (4). Let $\lambda_A^{(1)} \geq \lambda_A^{(2)} \geq \dots \geq \lambda_A^{(N_A)}$ and $\lambda_B^{(1)} \geq \lambda_B^{(2)} \geq \dots \geq \lambda_B^{(N_B)}$ be the eigenvalues of $\hat{\mathbf{R}}_A$ and $\hat{\mathbf{R}}_B$. Then we have

$$\begin{aligned} \log \mathbf{y}_l^H (\hat{\mathbf{R}}_A \otimes \hat{\mathbf{R}}_B)^{-1} \mathbf{y}_l &\geq \log \frac{\mathbf{y}_l^H (\hat{\mathbf{R}}_A \otimes \mathbf{I}_{N_B})^{-1} \mathbf{y}_l}{\lambda_B^{(1)}} \\ &\geq \frac{1}{N_B} \sum_{j=1}^{N_B} \log \mathbf{r}_{j,l}^H \hat{\mathbf{R}}_A^{-1} \mathbf{r}_{j,l} - \log \lambda_B^{(1)} + \log N_B, \end{aligned} \quad (54)$$

where we have utilized Jensen's inequality in the last step. Similarly, we have

$$\begin{aligned} \log \mathbf{y}_l^H (\hat{\mathbf{R}}_A \otimes \hat{\mathbf{R}}_B)^{-1} \mathbf{y}_l &\geq \frac{1}{N_A} \sum_{i=1}^{N_A} \log \mathbf{c}_{i,l}^H \hat{\mathbf{R}}_B^{-1} \mathbf{c}_{i,l} - \log \lambda_A^{(1)} + \log N_A. \end{aligned} \quad (55)$$

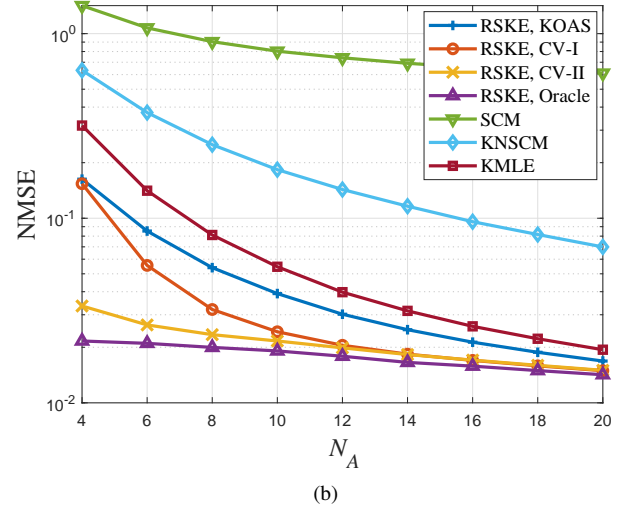
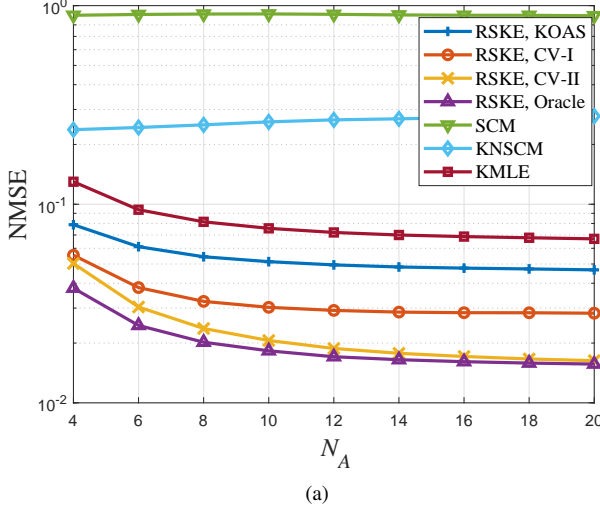


Fig. 4: NMSE versus the dimension. (a) $\epsilon_A = 0.1$ and $\epsilon_B = 0.9$; (b) $\epsilon_A = 0.9$ and $\epsilon_B = 0.1$.

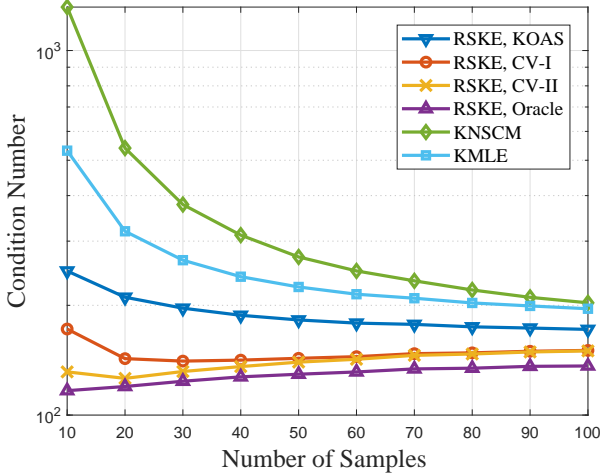


Fig. 5: Condition number versus the number of samples.

Here we have assumed that none of $\mathbf{r}_{j,l}$ and $\mathbf{c}_{i,l}$ is an all-zero vector, such that $\mathbf{r}_{j,l}^H \hat{\mathbf{R}}_A^{-1} \mathbf{r}_{j,l} \neq 0$, $\mathbf{c}_{i,l}^H \hat{\mathbf{R}}_B^{-1} \mathbf{c}_{i,l} \neq 0$, $\forall i, \forall j, \forall l$. Then let us define the following auxiliary functions:

$$\begin{aligned} \mathcal{F}_1(\hat{\mathbf{R}}_A) &= \frac{N_B L}{2} \log \det(\hat{\mathbf{R}}_A) + \frac{\beta_1 N_A}{2} \sum_{l=1}^L \sum_{j=1}^{N_B} \log \mathbf{r}_{j,l}^H \hat{\mathbf{R}}_A^{-1} \mathbf{r}_{j,l} \\ &\quad + \frac{\alpha_A L}{2} \text{Tr}(\hat{\mathbf{R}}_A^{-1}) + \frac{\alpha_A L}{2} \log \det(\hat{\mathbf{R}}_A) - \frac{\beta_2 L N}{2} \log \lambda_A^{(1)}, \end{aligned}$$

$$\begin{aligned} \mathcal{F}_2(\hat{\mathbf{R}}_B) &= \frac{N_A L}{2} \log \det(\hat{\mathbf{R}}_B) + \frac{\beta_2 N_B}{2} \sum_{l=1}^L \sum_{i=1}^{N_A} \log \mathbf{c}_{i,l}^H \hat{\mathbf{R}}_B^{-1} \mathbf{c}_{i,l} \\ &\quad + \frac{\alpha_B L}{2} \text{Tr}(\hat{\mathbf{R}}_B^{-1}) + \frac{\alpha_B L}{2} \log \det(\hat{\mathbf{R}}_B) - \frac{\beta_1 L N}{2} \log \lambda_B^{(1)}, \end{aligned}$$

where $\beta_1 + \beta_2 = 1$ and $\beta_1, \beta_2 \in [0, 1]$. From (54) and (55), we have

$$\begin{aligned} \mathcal{L}(\hat{\mathbf{R}}_A, \hat{\mathbf{R}}_B) &\geq \frac{2}{L} \left(\mathcal{F}_1(\hat{\mathbf{R}}_A) + \mathcal{F}_2(\hat{\mathbf{R}}_B) \right) + N(\beta_1 \log N_B + \beta_2 \log N_A). \end{aligned}$$

Since L, N, N_A and N_B are finite, if $\mathcal{F}_1(\hat{\mathbf{R}}_A) \rightarrow +\infty$ and $\mathcal{F}_2(\hat{\mathbf{R}}_B) \rightarrow +\infty$, then $\mathcal{L}(\hat{\mathbf{R}}_A, \hat{\mathbf{R}}_B) \rightarrow +\infty$. In the following, we check the conditions under which $\mathcal{F}_1(\hat{\mathbf{R}}_A) \rightarrow +\infty$ and $\mathcal{F}_2(\hat{\mathbf{R}}_B) \rightarrow +\infty$ on the boundary of the set of positive-definite, Hermitian matrices. Note that \mathcal{F}_1 and \mathcal{F}_2 are similar to the first equation of [36, Appendix A].

Denote the eigenvectors corresponding to $\lambda_A^{(i)}$ and $\lambda_B^{(j)}$ by $\mathbf{v}_A^{(i)}$ and $\mathbf{v}_B^{(j)}$, respectively, for $\hat{\mathbf{R}}_A$ and $\hat{\mathbf{R}}_B$. Then denote the subspace spanned by $\{\mathbf{v}_A^{(1)}, \dots, \mathbf{v}_A^{(i)}\}$ and $\{\mathbf{v}_B^{(1)}, \dots, \mathbf{v}_B^{(j)}\}$ as $\mathcal{S}_A^{(i)}$ and $\mathcal{S}_B^{(j)}$, respectively. Formally, define $\{r_A, s_A\}$ with $1 \leq r_A \leq s_A \leq N_A$, such that $\lambda_A^{(i)} \rightarrow \infty$ for $i \in [1, r_A]$, $\lambda_A^{(i)}$ is bounded for $i \in (r_A, s_A]$ and $\lambda_A^{(i)} \rightarrow 0$ for $i \in (s_A, N_A]$. Similarly, define $\{r_B, s_B\}$ for $\lambda_B^{(j)}$. Here we consider the case with $r_A \geq 1$, i.e., there exists at least one eigenvalue diverging, following [36], in order to examine the condition for $\mathcal{F}_1(\hat{\mathbf{R}}_A) \rightarrow +\infty$ at the boundary of feasible set for $\hat{\mathbf{R}}_A$.

Define $\mathcal{G}_1(\hat{\mathbf{R}}_A) = \exp(-\mathcal{F}_1(\hat{\mathbf{R}}_A))$ and $\mathcal{G}_2(\hat{\mathbf{R}}_B) = \exp(-\mathcal{F}_2(\hat{\mathbf{R}}_B))$. Clearly, $\mathcal{F}_1(\hat{\mathbf{R}}_A) \rightarrow +\infty$ is equivalent to $\mathcal{G}_1(\hat{\mathbf{R}}_A) \rightarrow 0$. From [36, Appendix A], the condition for $\mathcal{G}_1(\hat{\mathbf{R}}_A) \rightarrow 0$ can be checked by examining the infinitesimal equivalence of $\mathcal{G}_1(\hat{\mathbf{R}}_A)$ in terms of the eigenvalues $\lambda_A^{(i)}$ of $\hat{\mathbf{R}}_A$. From (36) in [36, Appendix A], $\mathcal{G}_1(\hat{\mathbf{R}}_A) \rightarrow 0$ if the orders of all the eigenvalues $\lambda_A^{(i)} \rightarrow \infty$ in the infinitesimal equivalence are negative and those of $\lambda_A^{(i)} \rightarrow 0$ are positive. Following this argument, we invoke (36) in [36, Appendix A] by letting $N = LN_B$, $K = N_A$, $\rho(s) = \frac{\beta_1 N_A}{2} \log(s)$, $h_1(s) = s$, $\alpha = \alpha_1 = \frac{\alpha_A L}{2}$ and $\mathbf{A}_1 = \mathbf{I}_{N_A}$, and hence $a_\rho = a'_\rho = \beta_1 N_A$ and $a_1 = +\infty$, $a'_1 = 0^2$. Note also that

² (a_ρ, a'_ρ) and (a_1, a'_1) are respectively defined for $\rho(s)$ and $\alpha h_1(s)$ according to [36, Definition 2]

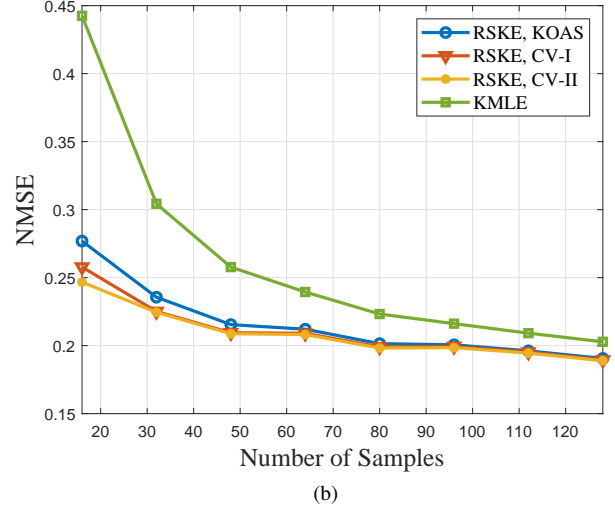
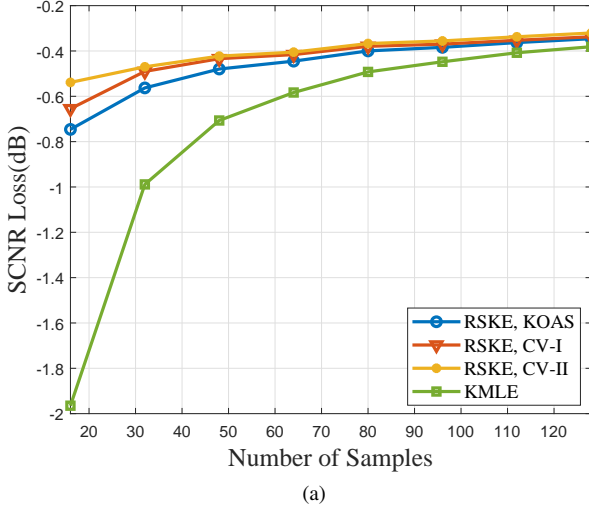


Fig. 6: The performance for the PSTAP application versus the sample number. (a) SCNR Loss; (b) NMSE.

for any $\epsilon > 0$,

$$(\lambda_A^{(1)})^{\frac{\beta_2 NL}{2}} = o\left((\varphi_A^{(1)})^{\frac{\beta_2 NL}{2}} - \epsilon\right) = o\left((\varphi_A^{(r)})^{\frac{\beta_2 NL}{2}} - \epsilon\right),$$

where $o(\cdot)$ denotes the higher order infinitesimal and $\varphi_A^{(i)} \triangleq (\lambda_A^{(i)})^{-1}$. Then we impose the same condition as the first line³ of (36) in [36, Appendix A], i.e.,

$$\left(\frac{LN_B}{2} + \frac{\alpha_A L}{2} - \epsilon\right)d - \frac{\beta_1 N_A + \epsilon}{2} LN_B P_{LN_B}(\mathcal{S}_A^{(d)}) - \frac{\beta_2 NL}{2} - \epsilon \geq 0, d = 1, \dots, N_A - 1.$$

Under this condition, $\mathcal{G}_1(\hat{\mathbf{R}}_A)$ goes to zero, i.e., $\mathcal{F}_1(\hat{\mathbf{R}}_A) \rightarrow +\infty$ on the boundary of positive-definite and Hermitian $\hat{\mathbf{R}}_A$ [36]. Letting $\epsilon \rightarrow 0$ and rearranging the terms, one has

$$P_{LN_B}(\mathcal{S}_A^{(d)}) < \frac{(LN_B + \alpha_A L)d - \beta_2 NL}{\beta_1 LN}, \quad (57)$$

for arbitrary $d = 1, \dots, N_A - 1$. Intuitively, this requires that the samples are evenly spread in the subspaces spanned by the eigenvectors of $\hat{\mathbf{R}}_A$. The condition (57) is then rewritten in a general form as (7a). Similarly, we have (7b).

In summary, we have obtained conditions (7a) and (7b) under which the cost function (4) tends to positive infinity at the boundary of the set of positive definite and Hermitian matrix. By [36, Lemma 1], these also give a sufficient condition that a solution to (5) exists.

APPENDIX B PROOF OF PROPOSITION 2

In this Appendix, we prove the convergence of the proposed iteration process, following the methodology of [36], [41]. By the concavity of the logarithm function, one has

³The second line of (36) in [36, Appendix A] is always met since $a_1 = +\infty$ in this paper.

$\log x \leq \log a + \frac{x}{a} - 1, \forall a > 0$. The equality holds when $x = a$. Then we have

$$\begin{aligned} \log \left[\mathbf{y}_l^H \left(\hat{\mathbf{R}}_A \otimes \hat{\mathbf{R}}_B^{(k)} \right)^{-1} \mathbf{y}_l \right] &\leq \frac{\mathbf{y}_l^H \left(\hat{\mathbf{R}}_A \otimes \hat{\mathbf{R}}_B^{(k)} \right)^{-1} \mathbf{y}_l}{\mathbf{y}_l^H \left(\hat{\mathbf{R}}_A^{(k)} \otimes \hat{\mathbf{R}}_B^{(k)} \right)^{-1} \mathbf{y}_l} \\ &+ \log \left[\mathbf{y}_l^H \left(\hat{\mathbf{R}}_A^{(k)} \otimes \hat{\mathbf{R}}_B^{(k)} \right)^{-1} \mathbf{y}_l \right] - 1, \end{aligned} \quad (58)$$

where the equality holds when $\hat{\mathbf{R}}_A = \hat{\mathbf{R}}_A^{(k)}$. We then construct the surrogate function

$$\begin{aligned} \mathcal{G}_1 \left(\hat{\mathbf{R}}_A \middle| \hat{\mathbf{R}}_A^{(k)}, \hat{\mathbf{R}}_B^{(k)} \right) &= \frac{N_B}{1 - \rho_A} \log \det \left(\hat{\mathbf{R}}_A \right) + \frac{N_A}{1 - \rho_B} \log \det \left(\hat{\mathbf{R}}_B^{(k)} \right) \\ &+ \frac{N}{L} \sum_{l=1}^L \frac{\mathbf{y}_l^H \left(\hat{\mathbf{R}}_A \otimes \hat{\mathbf{R}}_B^{(k)} \right)^{-1} \mathbf{y}_l}{\mathbf{y}_l^H \left(\hat{\mathbf{R}}_A^{(k)} \otimes \hat{\mathbf{R}}_B^{(k)} \right)^{-1} \mathbf{y}_l} \\ &+ \frac{N}{L} \sum_{l=1}^L \log \left[\mathbf{y}_l^H \left(\hat{\mathbf{R}}_A^{(k)} \otimes \hat{\mathbf{R}}_B^{(k)} \right)^{-1} \mathbf{y}_l \right] - N \\ &+ \frac{N_B \rho_A}{1 - \rho_A} \text{Tr} \left(\hat{\mathbf{R}}_A^{-1} \right) + \frac{N_A \rho_B}{1 - \rho_B} \text{Tr} \left(\left(\hat{\mathbf{R}}_B^{(k)} \right)^{-1} \right). \end{aligned} \quad (59)$$

Recalling (58), we have

$$\mathcal{L} \left(\hat{\mathbf{R}}_A, \hat{\mathbf{R}}_B^{(k)} \right) \leq \mathcal{G}_1 \left(\hat{\mathbf{R}}_A \middle| \hat{\mathbf{R}}_A^{(k)}, \hat{\mathbf{R}}_B^{(k)} \right), \quad (60)$$

and the equality holds when $\hat{\mathbf{R}}_A = \hat{\mathbf{R}}_A^{(k)}$, i.e.,

$$\mathcal{L} \left(\hat{\mathbf{R}}_A^{(k)}, \hat{\mathbf{R}}_B^{(k)} \right) = \mathcal{G}_1 \left(\hat{\mathbf{R}}_A^{(k)} \middle| \hat{\mathbf{R}}_A^{(k)}, \hat{\mathbf{R}}_B^{(k)} \right). \quad (61)$$

It is easy to verify that the minimizer of (59) is exactly (10a) by setting the gradient of (59) with respect to $\hat{\mathbf{R}}_A$ to zero. It follows that

$$\hat{\mathbf{R}}_A^{(k+1)} = \arg \min_{\hat{\mathbf{R}}_A} \mathcal{G}_1 \left(\hat{\mathbf{R}}_A \middle| \hat{\mathbf{R}}_A^{(k)}, \hat{\mathbf{R}}_B^{(k)} \right). \quad (62)$$

Therefore,

$$\begin{aligned}\mathcal{L}(\hat{\mathbf{R}}_A^{(k+1)}, \hat{\mathbf{R}}_B^{(k)}) &\leq \mathcal{G}_1\left(\hat{\mathbf{R}}_A^{(k+1)} \middle| \hat{\mathbf{R}}_A^{(k)}, \hat{\mathbf{R}}_B^{(k)}\right) \\ &= \min_{\hat{\mathbf{R}}_A} \mathcal{G}_1\left(\hat{\mathbf{R}}_A \middle| \hat{\mathbf{R}}_A^{(k)}, \hat{\mathbf{R}}_B^{(k)}\right) \leq \mathcal{G}_1\left(\hat{\mathbf{R}}_A^{(k)} \middle| \hat{\mathbf{R}}_A^{(k)}, \hat{\mathbf{R}}_B^{(k)}\right) \\ &= \mathcal{L}(\hat{\mathbf{R}}_A^{(k)}, \hat{\mathbf{R}}_B^{(k)}).\end{aligned}\quad (63)$$

Then define

$$\begin{aligned}\mathcal{G}_2\left(\hat{\mathbf{R}}_B \middle| \hat{\mathbf{R}}_A^{(k+1)}, \hat{\mathbf{R}}_B^{(k)}\right) &= \frac{N_B}{1-\rho_A} \log \det\left(\hat{\mathbf{R}}_A^{(k+1)}\right) + \frac{N_A}{1-\rho_B} \log \det\left(\hat{\mathbf{R}}_B\right) \\ &\quad + \frac{N}{L} \sum_{l=1}^L \frac{\mathbf{y}_l^H \left(\hat{\mathbf{R}}_A^{(k+1)} \otimes \hat{\mathbf{R}}_B\right)^{-1} \mathbf{y}_l}{\mathbf{y}_l^H \left(\hat{\mathbf{R}}_A^{(k+1)} \otimes \hat{\mathbf{R}}_B^{(k)}\right)^{-1} \mathbf{y}_l} \\ &\quad + \frac{N}{L} \sum_{l=1}^L \log \left[\mathbf{y}_l^H \left(\hat{\mathbf{R}}_A^{(k+1)} \otimes \hat{\mathbf{R}}_B^{(k)}\right)^{-1} \mathbf{y}_l \right] - N \\ &\quad + \frac{N_B \rho_A}{1-\rho_A} \text{Tr}\left(\left(\hat{\mathbf{R}}_A^{(k+1)}\right)^{-1}\right) + \frac{N_A \rho_B}{1-\rho_B} \text{Tr}\left(\hat{\mathbf{R}}_B^{-1}\right).\end{aligned}\quad (64)$$

Similarly, we can verify that the minimizer of (64) is exactly (10b), and

$$\mathcal{L}(\hat{\mathbf{R}}_A^{(k+1)}, \hat{\mathbf{R}}_B) \leq \mathcal{G}_2\left(\hat{\mathbf{R}}_B \middle| \hat{\mathbf{R}}_A^{(k+1)}, \hat{\mathbf{R}}_B^{(k)}\right), \quad (65)$$

where the equality holds when $\hat{\mathbf{R}}_B = \hat{\mathbf{R}}_B^{(k)}$, i.e.,

$$\mathcal{L}(\hat{\mathbf{R}}_A^{(k+1)}, \hat{\mathbf{R}}_B^{(k)}) = \mathcal{G}_2\left(\hat{\mathbf{R}}_B^{(k)} \middle| \hat{\mathbf{R}}_A^{(k+1)}, \hat{\mathbf{R}}_B^{(k)}\right). \quad (66)$$

It follows that

$$\begin{aligned}\mathcal{L}(\hat{\mathbf{R}}_A^{(k+1)}, \hat{\mathbf{R}}_B^{(k+1)}) &\leq \mathcal{G}_2\left(\hat{\mathbf{R}}_B^{(k+1)} \middle| \hat{\mathbf{R}}_A^{(k+1)}, \hat{\mathbf{R}}_B^{(k)}\right) \\ &= \min_{\hat{\mathbf{R}}_B} \mathcal{G}_2\left(\hat{\mathbf{R}}_B \middle| \hat{\mathbf{R}}_A^{(k+1)}, \hat{\mathbf{R}}_B^{(k)}\right) \leq \mathcal{G}_2\left(\hat{\mathbf{R}}_B^{(k)} \middle| \hat{\mathbf{R}}_A^{(k+1)}, \hat{\mathbf{R}}_B^{(k)}\right) \\ &= \mathcal{L}(\hat{\mathbf{R}}_A^{(k+1)}, \hat{\mathbf{R}}_B^{(k)}).\end{aligned}\quad (67)$$

Combining (63) and (67), we have

$$\mathcal{L}(\hat{\mathbf{R}}_A^{(k+1)}, \hat{\mathbf{R}}_B^{(k+1)}) \leq \mathcal{L}(\hat{\mathbf{R}}_A^{(k)}, \hat{\mathbf{R}}_B^{(k)}), \quad (68)$$

i.e., the penalized log-likelihood function $\mathcal{L}(\hat{\mathbf{R}}_A, \hat{\mathbf{R}}_B)$ in (4) is decreasing with iterations.

Since $\mathcal{L}(\hat{\mathbf{R}}_A, \hat{\mathbf{R}}_B)$ is g-convex, its minimizer exists and denote it by $(\hat{\mathbf{R}}_A^\infty, \hat{\mathbf{R}}_B^\infty)$. Then $\mathcal{L}(\hat{\mathbf{R}}_A^\infty, \hat{\mathbf{R}}_B^\infty)$ lower bounds the sequence $\{\mathcal{L}(\hat{\mathbf{R}}_A^{(k)}, \hat{\mathbf{R}}_B^{(k)}), k = 1, 2, \dots\}$. This indicates that the decreasing sequence $\{\mathcal{L}(\hat{\mathbf{R}}_A^{(k)}, \hat{\mathbf{R}}_B^{(k)})\}$ is bounded by an infimum. Then according to the monotone convergence theorem [80], the sequence will converge to the infimum as k increases, i.e., $(\hat{\mathbf{R}}_A^{(k)}, \hat{\mathbf{R}}_B^{(k)})$ will converge to the minimizer of $\mathcal{L}(\hat{\mathbf{R}}_A, \hat{\mathbf{R}}_B)$, i.e., the solution to (5).

APPENDIX C PROOF OF PROPOSITION 3

We here complete the proof by exploiting results from random matrix theory. Following [81], when the true covariance matrix \mathbf{R}_A and \mathbf{R}_B are known, the oracle shrinkage factor ρ_B^* , i.e., the solution to (15), is given by

$$\begin{aligned}\rho_B^* &= \frac{\mathbb{E}\left\{\text{Re}\left(\text{Tr}\left(\left(\mathbf{I}_{N_B} - \mathbf{C}_B\right)\left(\mathbf{R}_B - \mathbf{C}_B\right)^H\right)\right)\right\}}{\mathbb{E}\left\{\|\mathbf{I}_{N_B} - \mathbf{C}_B\|^2\right\}} \\ &= \frac{E_1 - E_2 - E_3 + \text{Tr}(\mathbf{R}_B)}{E_1 - 2E_2 + N_B},\end{aligned}\quad (69)$$

where $\text{Re}(\cdot)$ denotes the real part and

$$\begin{aligned}E_1 &= \mathbb{E}\left\{\text{Tr}(\mathbf{C}_B^2)\right\}, E_2 = \mathbb{E}\left\{\text{Re}(\text{Tr}(\mathbf{C}_B))\right\}, \\ E_3 &= \mathbb{E}\left\{\text{Re}(\text{Tr}(\mathbf{C}_B \mathbf{R}_B^H))\right\}\end{aligned}\quad (70)$$

and \mathbf{C}_B is defined by (30). The resulting optimal shrinkage estimate can be interpreted as the projection of the true CM onto the linear space spanned by \mathbf{C}_B and \mathbf{I}_{N_B} .

Let the eigendecompositions of \mathbf{R} , \mathbf{R}_A and \mathbf{R}_B be $\mathbf{R} = \mathbf{V} \mathbf{\Lambda} \mathbf{V}^H$, $\mathbf{R}_A = \mathbf{V}_A \mathbf{\Lambda}_A \mathbf{V}_A^H$, and $\mathbf{R}_B = \mathbf{V}_B \mathbf{\Lambda}_B \mathbf{V}_B^H$, respectively. Then, we define $\mathbf{z}_l = \frac{\mathbf{D}^{-1} \mathbf{y}_l}{\|\mathbf{D}^{-1} \mathbf{y}_l\|_2}$, where $\mathbf{D} = \mathbf{V} \mathbf{\Lambda}^{\frac{1}{2}}$. It is easy to see that $\|\mathbf{z}_l\|_2 = 1$ and $\{\mathbf{z}_l\}$ are independent of each other. Moreover, the whitened vectors $\{\mathbf{z}_l\}$ are isotropically distributed [82] and satisfy [33], [34]

$$\begin{aligned}\mathbb{E}\left\{\mathbf{z}_l \mathbf{z}_l^H\right\} &= \frac{1}{N} \mathbf{I}_N, \\ \mathbb{E}\left\{\left(\mathbf{z}_l^H \mathbf{\Lambda} \mathbf{z}_l\right)^2\right\} &= \frac{\text{Tr}(\mathbf{R}^2) + \text{Tr}^2(\mathbf{R})}{N(N+1)}, \\ \mathbb{E}\left\{\left(\mathbf{z}_l^H \mathbf{\Lambda} \mathbf{z}_q\right)^2\right\} &= \frac{1}{N^2} \text{Tr}(\mathbf{R}^2), l \neq q.\end{aligned}\quad (71)$$

Note that $\mathbf{D} = \mathbf{D}_A \otimes \mathbf{D}_B$, where $\mathbf{D}_A = \mathbf{V}_A \mathbf{\Lambda}_A^{\frac{1}{2}}$, $\mathbf{D}_B = \mathbf{V}_B \mathbf{\Lambda}_B^{\frac{1}{2}}$. We then reshape \mathbf{z}_l into a matrix satisfying

$$\mathbf{Z}_l = \text{unvec}_{N_B N_A}(\mathbf{z}_l) = \frac{\mathbf{D}_B^{-1} \mathbf{Y}_l (\mathbf{D}_A^{-1})^H}{\|\mathbf{D}^{-1} \mathbf{y}_l\|_2}, \quad (72)$$

which can be easily verified by vectorizing both sides of (72).

In order to determine the shrinkage factor for the robust shrinkage estimator of unstructured CM, [34] analyzed the feature of \mathbf{Z}_l where it reduces to a vector. We here extend the analysis to the more general case of matrix-valued \mathbf{Z}_l by exploiting random matrix theory and properties of Kronecker product. Let $z_l^{(i)}$ be the i th entry of \mathbf{z}_l . From (71), one has

$$\mathbb{E}\left\{z_l^{(i)} \left(z_l^{(j)}\right)^*\right\} = \begin{cases} 1/N & i = j \\ 0 & i \neq j \end{cases}. \quad (73)$$

This indicates that $\{z_l^{(i)}\}_{i=1}^N$ are i.i.d. with zero mean and variance $1/N$. Consequently, we have

$$\mathbb{E}\left\{\mathbf{Z}_l \mathbf{Z}_l^H\right\} = \frac{N_A}{N} \mathbf{I}_{N_B}, \mathbb{E}\left\{\mathbf{Z}_l^H \mathbf{Z}_l\right\} = \frac{N_B}{N} \mathbf{I}_{N_A}. \quad (74)$$

Note that $\|\mathbf{D}^{-1} \mathbf{y}_l\|_2^2 = \mathbf{y}_l^H (\mathbf{R}_A \otimes \mathbf{R}_B)^{-1} \mathbf{y}_l$, and we have

$$\begin{aligned}\frac{\mathbf{Y}_l \mathbf{R}_A^{-1} \mathbf{Y}_l^H}{\mathbf{y}_l^H (\mathbf{R}_A \otimes \mathbf{R}_B)^{-1} \mathbf{y}_l} &= \mathbf{D}_B \mathbf{Z}_l \mathbf{Z}_l^H \mathbf{D}_B^H, \\ \frac{\mathbf{Y}_l^H \mathbf{R}_B^{-1} \mathbf{Y}_l}{\mathbf{y}_l^H (\mathbf{R}_A \otimes \mathbf{R}_B)^{-1} \mathbf{y}_l} &= \mathbf{D}_A \mathbf{Z}_l^H \mathbf{Z}_l \mathbf{D}_A^H,\end{aligned}\quad (75)$$

Note that $\mathbb{E}\{\cdot\}$, $\text{Re}(\cdot)$ and $\text{Tr}(\cdot)$ are exchangeable to each other. Substituting (75) into (70), one has

$$E_2 = \text{Tr} \left(\frac{N}{LN_A} \sum_{l=1}^L \mathbf{D}_B \mathbb{E}(\mathbf{Z}_l \mathbf{Z}_l^H) \mathbf{D}_B^H \right) = \text{Tr}(\mathbf{R}_B), \quad (76)$$

$$E_3 = \text{Tr}(\mathbf{R}_B^2),$$

From [83], [84], we have

$$\mathbb{E} \left\{ \left| z_l^{(i)} \right|^4 \right\} = \frac{2}{N(N+1)}, \mathbb{E} \left\{ \left| z_l^{(i)} \right|^2 \left| z_l^{(j)} \right|^2 \right\} = \frac{1}{N(N+1)}. \quad (77)$$

Since $\{\mathbf{z}_l\}_{l=1}^L$ are i.i.d, we have

$$\mathbb{E} \left\{ \left| z_l^{(i)} \right|^2 \left| z_q^{(j)} \right|^2 \right\} = \frac{1}{N^2}, \mathbb{E} \left\{ z_q^{(i)} \left(z_l^{(i)} \right)^* z_l^{(j)} \left(z_q^{(j)} \right)^* \right\} = 0. \quad (78)$$

Therefore, (70) can be rewritten as

$$\begin{aligned} E_1 &= \mathbb{E} \left\{ \text{Tr}(\mathbf{C}_B^2) \right\} \\ &= \left(\frac{N}{LN_A} \right)^2 \mathbb{E} \left\{ \text{Tr} \left(\sum_{l=1}^L \sum_{q=1}^L \mathbf{D}_B \mathbf{Z}_l \mathbf{Z}_l^H \mathbf{D}_B^H \mathbf{D}_B \mathbf{Z}_q \mathbf{Z}_q^H \mathbf{D}_B^H \right) \right\} \\ &= \left(\frac{N}{LN_A} \right)^2 \mathbb{E} \left\{ \sum_{l=1}^L \sum_{q=1}^L \text{Tr}(\mathbf{Z}_l^H \mathbf{\Lambda}_B \mathbf{Z}_q \mathbf{Z}_q^H \mathbf{\Lambda}_B \mathbf{Z}_l) \right\}. \end{aligned} \quad (79)$$

Utilizing [83, Lemma 1.1] and substituting (77), (78) into (79), E_1 is obtained as (80) in the following page. Substituting (80) and (76) into (69), (17b) is obtained. Similarly, we can have the optimal ρ_A^* , i.e., (17a). The resulting expressions of ρ_A^* and ρ_B^* can be used to produce the KOAS choice $\rho_{A,\text{KOAS}}$ and $\rho_{B,\text{KOAS}}$ by plugging estimates of \mathbf{R}_A and \mathbf{R}_B into (17).

APPENDIX D PROOF OF PROPOSITION 4

This proposition can be proven by combining the results in Appendix C. Recalling (19), (74) and (75), we have

$$\begin{aligned} \mathbb{E}(\mathbf{S}_A) &= N_A \mathbf{D}_A \mathbb{E}(\mathbf{Z}_l^H \mathbf{Z}_l) \mathbf{D}_A^H = \mathbf{R}_A, \\ \mathbb{E}(\mathbf{S}_B) &= N_B \mathbf{D}_B \mathbb{E}(\mathbf{Z}_l \mathbf{Z}_l^H) \mathbf{D}_B^H = \mathbf{R}_B. \end{aligned} \quad (81)$$

Moreover, (18) can be rewritten as

$$\mathcal{J}_A(\mathbf{\Sigma}_A) = \text{Tr}(\mathbf{\Sigma}_A^2 - 2\text{Re}(\mathbf{\Sigma}_A \mathbb{E}(\mathbf{S}_A)) + \mathbb{E}(\mathbf{S}_A^2)), \quad (82a)$$

$$\mathcal{J}_B(\mathbf{\Sigma}_B) = \text{Tr}(\mathbf{\Sigma}_B^2 - 2\text{Re}(\mathbf{\Sigma}_B \mathbb{E}(\mathbf{S}_B)) + \mathbb{E}(\mathbf{S}_B^2)). \quad (82b)$$

By setting the derivative of (82a) and (82b) with respect to $\mathbf{\Sigma}_A$ and $\mathbf{\Sigma}_B$ to zero, we have the minimizer of (18) as $\mathbf{\Sigma}_A = \mathbf{R}_A$ and $\mathbf{\Sigma}_B = \mathbf{R}_B$.

REFERENCES

- [1] G. Noriega and S. Pasupathy, "Adaptive estimation of noise covariance matrices in real-time preprocessing of geophysical data," *IEEE Transactions on Geoscience and Remote Sensing*, vol. 35, no. 5, pp. 1146–1159, 1997.
- [2] S. Tadjudin and D. A. Landgrebe, "Covariance estimation with limited training samples," *IEEE Transactions on Geoscience and Remote Sensing*, vol. 37, no. 4, pp. 2113–2118, 1999.
- [3] I. S. Reed, J. D. Mallett, and L. E. Brennan, "Rapid convergence rate in adaptive arrays," *IEEE Transactions on Aerospace and Electronic Systems*, vol. 10, no. 6, pp. 853–863, Nov 1974.
- [4] P. J. Bickel, E. Levina *et al.*, "Regularized estimation of large covariance matrices," *The Annals of Statistics*, vol. 36, no. 1, pp. 199–227, 2008.
- [5] P. Chen, W. L. Melvin, and M. C. Wicks, "Screening among multivariate normal data," *Journal of Multivariate Analysis*, vol. 69, no. 1, pp. 10–29, 1999.
- [6] E. J. Kelly, "An adaptive detection algorithm," *IEEE Transactions on Aerospace and Electronic Systems*, vol. 22, no. 2, pp. 115–127, March 1986.
- [7] J. B. Billingsley, "Ground clutter measurements for surface-sited radar," NASA STI/Recon Technical Report N, p. 28655, Feb. 1993.
- [8] M. Rangaswamy, "Statistical analysis of the nonhomogeneity detector for non-gaussian interference backgrounds," *IEEE Transactions on Signal Processing*, vol. 53, no. 6, pp. 2101–2111, 2005.
- [9] F. Gini and A. Farina, "Vector subspace detection in compound-gaussian clutter. part i: survey and new results," *IEEE Transactions on Aerospace and Electronic Systems*, vol. 38, no. 4, pp. 1295–1311, 2002.
- [10] E. Ollila, D. E. Tyler, V. Koivunen, and H. V. Poor, "Complex elliptically symmetric distributions: Survey, new results and applications," *IEEE Transactions on Signal Processing*, vol. 60, no. 11, pp. 5597–5625, Nov 2012.
- [11] C. J. Baker, "K-distributed coherent sea clutter," *IEE Proceedings F - Radar and Signal Processing*, vol. 138, no. 2, pp. 89–92, 1991.
- [12] E. Conte and M. Longo, "Characterisation of radar clutter as a spherically invariant random process," *IEE Proceedings F - Communications, Radar and Signal Processing*, vol. 134, no. 2, pp. 191–197, April 1987.
- [13] K. J. Sangston, F. Gini, M. V. Greco, and A. Farina, "Structures for radar detection in compound gaussian clutter," *IEEE Transactions on Aerospace and Electronic Systems*, vol. 35, no. 2, pp. 445–458, 1999.
- [14] J. B. Billingsley, A. Farina, F. Gini, M. V. Greco, and L. Verrazzani, "Statistical analyses of measured radar ground clutter data," *IEEE Transactions on Aerospace and Electronic Systems*, vol. 35, no. 2, pp. 579–593, April 1999.
- [15] Y. Wu, T. Wang, J. Wu, and J. Duan, "Training sample selection for space-time adaptive processing in heterogeneous environments," *IEEE Geoscience and Remote Sensing Letters*, vol. 12, no. 4, pp. 691–695, 2014.
- [16] A. Aubry, A. D. Maio, L. Pallotta, and A. Farina, "Median matrices and their application to radar training data selection," *IET Radar, Sonar Navigation*, vol. 8, no. 4, pp. 265–274, 2014.
- [17] Q. Zhang, Y. Tian, Y. Yang, and C. Pan, "Automatic spatial-spectral feature selection for hyperspectral image via discriminative sparse multimodal learning," *IEEE Transactions on Geoscience and Remote Sensing*, vol. 53, no. 1, pp. 261–279, 2015.
- [18] Y. Tarabalka, J. A. Benediktsson, J. Chanussot, and J. C. Tilton, "Multiple spectral-spatial classification approach for hyperspectral data," *IEEE Transactions on Geoscience and Remote Sensing*, vol. 48, no. 11, pp. 4122–4132, 2010.
- [19] Y. Bazi and F. Melgani, "Toward an optimal svm classification system for hyperspectral remote sensing images," *IEEE Transactions on Geoscience and Remote Sensing*, vol. 44, no. 11, pp. 3374–3385, 2006.
- [20] G. Cui, N. Li, L. Pallotta, G. Foglia, and L. Kong, "Geometric barycenters for covariance estimation in compound-gaussian clutter," *IET Radar, Sonar Navigation*, vol. 11, no. 3, pp. 404–409, 2017.
- [21] M. Li, G. Sun, J. Tong, and Z. He, "Covariance matrix whitening-based training sample selection method for airborne radar," *IEEE Geoscience and Remote Sensing Letters*, pp. 1–5, 2020.
- [22] S. Han, A. De Maio, V. Carotenuto, L. Pallotta, and X. Huang, "Censoring outliers in radar data: An approximate ml approach and its analysis," *IEEE Transactions on Aerospace and Electronic Systems*, vol. 55, no. 2, pp. 534–546, 2019.
- [23] Huber and J. Peter, "Robust estimation of a location parameter," *Annals of Mathematical Statistics*, vol. 35, no. 1, pp. 73–101, 1964.
- [24] F. R. Hampel, "The influence curve and its role in robust estimation," *Journal of the American Statistical Association*, vol. 69, no. 346, pp. 383–393, 1974.

$$\begin{aligned}
E_1 &= \left(\frac{N}{LN_A} \right)^2 \mathbb{E} \left\{ \sum_{l=1}^L \sum_{q=1}^L \sum_{i=1}^{N_A} \sum_{k=1}^{N_A} \sum_{m=1}^{N_B} \sum_{n=1}^{N_B} \left(\lambda_B^{(m)} \lambda_B^{(n)} z_q^{(N_B(k-1)+m)} \left(z_l^{(N_B(i-1)+m)} \right)^* z_l^{(N_B(i-1)+n)} \left(z_q^{(N_B(k-1)+n)} \right)^* \right) \right\} \\
&= \left(\frac{N}{LN_A} \right)^2 \left[\left(\frac{2N_AL}{N(N+1)} + \frac{N_AL(L-1)}{N^2} + \frac{N_A(N_A-1)L}{N(N+1)} + \frac{N_A(N_A-1)L(L-1)}{N^2} \right) \left(\sum_{m=1}^{N_B} \left(\lambda_B^{(m)} \right)^2 \right) \right. \\
&\quad \left. + \left(\frac{N_AL}{N(N+1)} \right) \left(\sum_{m \neq n} \lambda_B^{(m)} \lambda_B^{(n)} \right) \right] = \left(1 - \frac{1}{L(N+1)} \right) \text{Tr}(\mathbf{R}_B^2) + \left(\frac{N}{N_AL(N+1)} \right) \text{Tr}^2(\mathbf{R}_B).
\end{aligned} \tag{80}$$

- [25] D. E. Tyler, "A distribution-free M-estimator of multivariate scatter," *The Annals of Statistics*, vol. 15, no. 1, pp. 234–251, 1987.
- [26] R. A. Maronna, "Robust M-estimators of multivariate location and scatter," *The Annals of Statistics*, vol. 4, no. 1, pp. 51–67, 1976.
- [27] F. Pascal, Y. Chitour, J. Ovarlez, P. Forster, and P. Larzabal, "Covariance structure maximum-likelihood estimates in compound Gaussian noise: Existence and algorithm analysis," *IEEE Transactions on Signal Processing*, vol. 56, no. 1, pp. 34–48, Jan 2008.
- [28] M. Mahot, F. Pascal, P. Forster, and J. Ovarlez, "Asymptotic properties of robust complex covariance matrix estimates," *IEEE Transactions on Signal Processing*, vol. 61, no. 13, pp. 3348–3356, 2013.
- [29] M. Greco and F. Gini, "Cramér-Rao lower bounds on covariance matrix estimation for complex elliptically symmetric distributions," *IEEE Transactions on Signal Processing*, vol. 61, no. 24, pp. 6401–6409, 2013.
- [30] J. P. Hoffbeck and D. A. Landgrebe, "Covariance matrix estimation and classification with limited training data," *IEEE Transactions on Pattern Analysis and Machine Intelligence*, vol. 18, no. 7, pp. 763–767, July 1996.
- [31] O. Ledoit and M. Wolf, "A well-conditioned estimator for large-dimensional covariance matrices," *Journal of Multivariate Analysis*, vol. 88, no. 2, pp. 365–411, 2004.
- [32] P. Stoica, J. Li, X. Zhu, and J. R. Guerci, "On using a priori knowledge in Space-Time Adaptive Processing," *IEEE Transactions on Signal Processing*, vol. 56, no. 6, pp. 2598–2602, June 2008.
- [33] Y. Chen, A. Wiesel, Y. C. Eldar, and A. O. Hero, "Shrinkage algorithms for MMSE covariance estimation," *IEEE Transactions on Signal Processing*, vol. 58, no. 10, pp. 5016–5029, Oct 2010.
- [34] Y. Chen, A. Wiesel, and A. O. Hero, "Robust shrinkage estimation of high-dimensional covariance matrices," *IEEE Transactions on Signal Processing*, vol. 59, no. 9, pp. 4097–4107, Sep. 2011.
- [35] F. Pascal, Y. Chitour, and Y. Quek, "Generalized robust shrinkage estimator and its application to STAP detection problem," *IEEE Transactions on Signal Processing*, vol. 62, no. 21, pp. 5640–5651, Nov 2014.
- [36] Y. Sun, P. Babu, and D. P. Palomar, "Regularized Tyler's scatter estimator: Existence, uniqueness, and algorithms," *IEEE Transactions on Signal Processing*, vol. 62, no. 19, pp. 5143–5156, Oct 2014.
- [37] E. Ollila and D. E. Tyler, "Regularized M-Estimators of scatter matrix," *IEEE Transactions on Signal Processing*, vol. 62, no. 22, pp. 6059–6070, Nov 2014.
- [38] S. Arlot, A. Celisse *et al.*, "A survey of cross-validation procedures for model selection," *Statistics surveys*, vol. 4, pp. 40–79, 2010.
- [39] J. Tong, R. Hu, J. Xi, Z. Xiao, Q. Guo, and Y. Yu, "Linear shrinkage estimation of covariance matrices using low-complexity cross-validation," *Signal Processing*, vol. 148, pp. 223–233, 2018.
- [40] J. Tong, P. J. Schreier, Q. Guo, S. Tong, J. Xi, and Y. Yu, "Shrinkage of covariance matrices for linear signal estimation using cross-validation," *IEEE Transactions on Signal Processing*, vol. 64, no. 11, pp. 2965–2975, June 2016.
- [41] A. Wiesel, "Geodesic convexity and covariance estimation," *IEEE Transactions on Signal Processing*, vol. 60, no. 12, pp. 6182–6189, 2012.
- [42] Y. Sun, P. Babu, and D. P. Palomar, "Robust estimation of structured covariance matrix for heavy-tailed elliptical distributions," *IEEE Transactions on Signal Processing*, vol. 64, no. 14, pp. 3576–3590, July 2016.
- [43] A. De Maio, L. Pallotta, J. Li, and P. Stoica, "Loading factor estimation under affine constraints on the covariance eigenvalues with application to radar target detection," *IEEE Transactions on Aerospace and Electronic Systems*, vol. 55, no. 3, pp. 1269–1283, 2019.
- [44] Y. I. Abramovich and O. Besson, "Regularized covariance matrix estimation in complex elliptically symmetric distributions using the expected likelihood approach— part 1: The over-sampled case," *IEEE Transactions on Signal Processing*, vol. 61, no. 23, pp. 5807–5818, 2013.
- [45] X. Du, A. Aubry, A. De Maio, and G. Cui, "Toeplitz structured covariance matrix estimation for radar applications," *IEEE Signal Processing Letters*, vol. 27, pp. 595–599, 2020.
- [46] J. Li, A. Aubry, A. De Maio, and J. Zhou, "An el approach for similarity parameter selection in ka covariance matrix estimation," *IEEE Signal Processing Letters*, vol. 26, no. 8, pp. 1217–1221, 2019.
- [47] A. Aubry, V. Carotenuto, A. D. Maio, and G. Foglia, "Exploiting multiple a priori spectral models for adaptive radar detection," *IET Radar, Sonar Navigation*, vol. 8, no. 7, pp. 695–707, 2014.
- [48] M. Steiner and K. Gerlach, "Fast converging adaptive processor or a structured covariance matrix," *IEEE Transactions on Aerospace and Electronic Systems*, vol. 36, no. 4, pp. 1115–1126, Oct 2000.
- [49] A. Aubry, A. De Maio, and V. Carotenuto, "Optimality claims for the fml covariance estimator with respect to two matrix norms," *IEEE Transactions on Aerospace and Electronic Systems*, vol. 49, no. 3, pp. 2055–2057, 2013.
- [50] G. Sun, Z. He, J. Tong, and X. Zhang, "Knowledge-aided covariance matrix estimation via Kronecker product expansions for airborne STAP," *IEEE Geoscience and Remote Sensing Letters*, vol. 15, no. 4, pp. 527–531, April 2018.
- [51] G. Sun, M. Li, J. Tong, and Y. Ji, "Structured clutter covariance matrix estimation for airborne mimo radar with limited training data," *IEEE Geoscience and Remote Sensing Letters*, pp. 1–5, 2020.
- [52] J. P. Kermoal, L. Schumacher, K. I. Pedersen, P. E. Mogensen, and F. Frederiksen, "A stochastic MIMO radio channel model with experimental validation," *IEEE Journal on Selected Areas in Communications*, vol. 20, no. 6, pp. 1211–1226, Aug 2002.
- [53] Kai Yu, M. Bengtsson, B. Ottersten, D. McNamara, P. Karlsson, and M. Beach, "Modeling of wide-band MIMO radio channels based on NLoS indoor measurements," *IEEE Transactions on Vehicular Technology*, vol. 53, no. 3, pp. 655–665, May 2004.
- [54] K. Werner, M. Jansson, and P. Stoica, "On estimation of covariance matrices with Kronecker product structure," *IEEE Transactions on Signal Processing*, vol. 56, no. 2, pp. 478–491, Feb 2008.
- [55] G. Alfano, A. D. Maio, and E. Conte, "Polarization diversity detection of distributed targets in compound-Gaussian clutter," *IEEE Transactions on Aerospace and Electronic Systems*, vol. 40, no. 2, pp. 755–765, April 2004.
- [56] J. Liu, W. Liu, B. Chen, H. Liu, H. Li, and C. Hao, "Modified Rao test for multichannel adaptive signal detection," *IEEE Transactions on Signal Processing*, vol. 64, no. 3, pp. 714–725, Feb 2016.
- [57] G. Cui, L. Kong, X. Yang, and J. Yang, "Distributed target detection with polarimetric MIMO radar in compound-Gaussian clutter," *Digital Signal Processing*, vol. 22, no. 3, pp. 430–438, 2012.
- [58] L. Xie, Z. He, J. Tong, J. Li, and H. Li, "Transmitter polarization optimization for space-time adaptive processing with diversely polarized antenna array," *Signal Processing*, vol. 169, p. 107401, 2020.
- [59] N. Lu and D. L. Zimmerman, "The likelihood ratio test for a separable covariance matrix," *Statistics Probability Letters*, vol. 73, no. 4, pp. 449–457, 2005.
- [60] Y. Wang, W. Xia, Z. He, H. Li, and A. P. Petropulu, "Polarimetric detection in compound gaussian clutter with Kronecker structured covariance matrix," *IEEE Transactions on Signal Processing*, vol. 65, no. 17, pp. 4562–4576, Sept 2017.
- [61] A. B. Kostinski and A. C. Koivunen, "On the condition number of gaussian sample-covariance matrices," *IEEE Transactions on Geoscience and Remote Sensing*, vol. 38, no. 1, pp. 329–332, 2000.

- [62] Y. Sun, P. Babu, and D. P. Palomar, "Majorization-minimization algorithms in signal processing, communications, and machine learning," *IEEE Transactions on Signal Processing*, vol. 65, no. 3, pp. 794–816, Feb 2017.
- [63] A. Wiesel, T. Zhang *et al.*, "Structured robust covariance estimation," *Foundations and Trends in Signal Processing*, vol. 8, no. 3, pp. 127–216, 2015.
- [64] L. C. Godara, "Application of antenna arrays to mobile communications. II. Beam-forming and direction-of-arrival considerations," *Proceedings of the IEEE*, vol. 85, no. 8, pp. 1195–1245, 1997.
- [65] E. A. P. Habets, J. Benesty, I. Cohen, S. Gannot, and J. Dmochowski, "New insights into the mvdr beamformer in room acoustics," *IEEE Transactions on Audio, Speech, and Language Processing*, vol. 18, no. 1, pp. 158–170, 2009.
- [66] J. Ward, "Space-time adaptive processing for airborne radar," in *1995 International Conference on Acoustics, Speech, and Signal Processing*, vol. 5, May 1995, pp. 2809–2812 vol.5.
- [67] R. Klemm, *Principles of Space-Time Adaptive Processing*, 01 2006.
- [68] W. L. Melvin, "A STAP overview," *IEEE Aerospace and Electronic Systems Magazine*, vol. 19, no. 1, pp. 19–35, Jan 2004.
- [69] L. Xie, Z. He, J. Tong, and W. Zhang, "A recursive angle-doppler channel selection method for reduced-dimension space-time adaptive processing," *IEEE Transactions on Aerospace and Electronic Systems*, vol. 56, no. 5, pp. 3985–4000, Oct 2020.
- [70] J. V. Davis, B. Kulis, P. Jain, S. Sra, and I. S. Dhillon, "Information-theoretic metric learning," in *Proceedings of the 24th international conference on Machine learning*, 2007, pp. 209–216.
- [71] I. S. Dhillon, "The log-determinant divergence and its applications," in *Householder Symposium XVII, Zeuthen, Germany*, 2008.
- [72] D. R. Hunter and K. Lange, "A tutorial on MM algorithms," *The American Statistician*, vol. 58, no. 1, pp. 30–37, 2004.
- [73] M. Hurtado and A. Nehorai, "Polarimetric detection of targets in heavy inhomogeneous clutter," *IEEE Transactions on Signal Processing*, vol. 56, no. 4, pp. 1349–1361, April 2008.
- [74] A. De Maio, "Robust adaptive radar detection in the presence of steering vector mismatches," *IEEE Transactions on Aerospace and Electronic Systems*, vol. 41, no. 4, pp. 1322–1337, Oct 2005.
- [75] L. M. Novak, M. C. Burl, and W. W. Irving, "Optimal polarimetric processing for enhanced target detection," *IEEE Transactions on Aerospace and Electronic Systems*, vol. 29, no. 1, pp. 234–244, Jan 1993.
- [76] A. M. Haimovich and Y. Bar-Ness, "An eigenanalysis interference canceler," *IEEE Transactions on Signal Processing*, vol. 39, no. 1, pp. 76–84, 1991.
- [77] M. G. Amin, X. Wang, Y. D. Zhang, F. Ahmad, and E. Aboutanios, "Sparse arrays and sampling for interference mitigation and doa estimation in gnss," *Proceedings of the IEEE*, vol. 104, no. 6, pp. 1302–1317, 2016.
- [78] J. S. Goldstein and I. S. Reed, "Theory of partially adaptive radar," *IEEE Transactions on Aerospace and Electronic Systems*, vol. 33, no. 4, pp. 1309–1325, Oct 1997.
- [79] A. Breloy, G. Ginolhac, F. Pascal, and P. Forster, "Robust covariance matrix estimation in heterogeneous low rank context," *IEEE Transactions on Signal Processing*, vol. 64, no. 22, pp. 5794–5806, Nov 2016.
- [80] J. Bibby, "Axiomatisations of the average and a further generalisation of monotonic sequences," *Glasgow Mathematical Journal*, vol. 15, no. 1, p. 63–65, 1974.
- [81] O. Ledoit and M. Wolf, "Improved estimation of the covariance matrix of stock returns with an application to portfolio selection," *Journal of Empirical Finance*, vol. 10, no. 5, pp. 603 – 621, 2003.
- [82] T. L. Marzetta and B. M. Hochwald, "Capacity of a mobile multiple-antenna communication link in Rayleigh flat fading," *IEEE Transactions on Information Theory*, vol. 45, no. 1, pp. 139–157, Jan 1999.
- [83] F. Hiai and D. Petz, "Asymptotic freeness almost everywhere for random matrices," *Acta Sci. Math. Szeged*, vol. 66, pp. 801–826, 2000.
- [84] A. M. Tulino, S. Verdú *et al.*, "Random matrix theory and wireless communications," *Foundations and Trends in Communications and Information Theory*, vol. 1, no. 1, pp. 1–182, 2004.